Journal of Materials Chemistry A

REVIEW

View Article Online
View Journal | View Issue

Cite this: J. Mater. Chem. A, 2019, 7, 25227

Emerging two-dimensional noncarbon nanomaterials for flexible lithium-ion batteries: opportunities and challenges

Yan Li,[a] Renheng Wang,*[a] Zhinan Guo,[a] Zhe Xiao,[a] Huide Wang,[a] Xiaoling Luo*[b] and Han Zhang *[a]

Received 26th August 2019
Accepted 16th October 2019

DOI: 10.1039/c9ta09377j

rsc.li/materials-a

The flexible electronics technology revolution is driven ever forward by a strong demand for portable, wearable and lightweight electronic products in the market. Flexible lithium-ion batteries (LIBs) have attracted considerable attention because of their excellent electrochemical and mechanical properties. Due to the particular folded structure, high electrical conductivity and excellent flexibility, several emerging two-dimensional (2D) noncarbon nanomaterials such as phosphorene, borophene, MoS_2, $Ti_3C_2T_x$ and V_2O_5 have been widely applied to flexible LIBs with bright prospects. This review examines the existing literature and recent advances of flexible LIBs based on 2D materials, covering the classifications, synthetic methods and merits of emerging 2D noncarbon nanomaterials. Theoretical research and practical applications of emerging 2D noncarbon nanomaterials as electrode materials for flexible LIBs are reviewed as well. In addition, challenges faced by emerging 2D noncarbon nanomaterials are summarized and prospects of these 2D nanomaterials are given in order to broaden their potential in flexible LIBs.

1. Introduction

With consumer trends pushing toward portable and wearable electronic products, the concept of flexible devices emerges at the right moment and engulfs the entire world.[1–4] One of the biggest obstacles to the application of flexible electronic products is the development of flexible energy storage devices.[5–8] LIBs have unique advantages when applied to electronic devices due to their numerous advantages such as low weight, small

[a]Institute of Microscale Optoelectronics, Collaborative Innovation Centre for Optoelectronic Science & Technology, Key Laboratory of Optoelectronic Devices and Systems of Ministry of Education and Guangdong Province, College of Physics and Optoelectronic Engineering, Shenzhen Key Laboratory of Micro-Nano Photonic Information Technology, Guangdong Laboratory of Artificial Intelligence and Digital Economy (SZ), Shenzhen University, Shenzhen 518060, P. R. China. E-mail: hzhang@szu.edu.cn; wangrh@szu.edu.cn

[b]Department of Ophthalmology, Shenzhen People's Hospital, Second Clinical Medical College of Jinan University, Shenzhen City, Guangdong Province, 518020, People's Republic of China. E-mail: LXL2603@vip.sina.com

Yan Li received her Ph.D. degree in Metallurgical Engineering from Central South University (CSU) in 2018. From July 2018, she has been working as a postdoctoral fellow in Shenzhen University. Her research interests include the synthesis and modification of cathode and anode materials for lithium ion batteries, and the synthesis and application of low-dimensional nanomaterials for flexible lithium ion batteries.

Renheng Wang received his Ph.D. degree in Metallurgical Engineering from Central South University (CSU) in 2015. From January 2016 to October 2018, he worked as a postdoctoral fellow at Shenzhen University and Nanyang Technological University. He is now a researcher at the College of Physics and Optoelectronic Engineering, Shenzhen University. His research focuses on the synthesis and application of nanomaterials and composites for clean energy storage, such as high-power/high-energy lithium ion batteries.

size, high specific power, high energy density, excellent recycling ability and superior rate performance.[9–15] However, the separation of electrode materials and the current collector affects the electrochemical properties when traditional rigid LIBs are folded, and even leads to short circuit and other serious safety problems.[16–18] Consequently, it is of profound significance to endow LIBs with flexibility and develop electrodes with high flexibility and excellent electrochemical performance for realizing flexible electronics. In the initial studies, various flexible matrixes such as polymers, paper and textiles are prepared to replace traditional copper foil and aluminum foil as current collectors for carrying the active materials in flexible LIBs.[19–24] However, these non-electroactive matrixes with low conductivity greatly affect the quick charge–discharge process of batteries and degrade the electrochemical performance. Therefore, flexible electrodes with a conductive matrix such as graphene, carbon fiber paper and carbon nanotube films have become a hot research topic.[25–30] In addition, many researchers have proposed to build 3D thin-film electrodes which were formed by combining traditional active electrode materials with flexible carbon-based materials. Carbon-based materials act as not only the basic element of the conductive network, but also the supporting framework of the whole electrode.[31–34] This method can fully combine the advantages of carbon-based materials and traditional active electrode materials. However, the intrinsic rigidity of traditional active materials significantly limits the flexibility of the whole electrode, and thus flexible LIBs still face a huge challenge in possessing both strong flexibility and good electrochemical properties.

One of the gravest challenges confronting fully flexible energy storage devices is to research and develop electrode materials with both desirable electrochemical properties and mechanical performance. Recently, 2D nanomaterials have been widely employed in research for electronics,[35–42] optoelectronics,[43–69] catalysis,[70,71] supercapacitors,[21] sensors,[72–76] biological medicine[77–79] and energy devices[14,80] due to their attractive qualities including tunable direct band gaps, wide interlayer distances, high mobilities and remarkable mechanical strength.[81] The particular structure of 2D nanomaterials leads to their huge specific surface area, good conductivity, natural flexibility and high lithium storage capacity, thus attracting considerable attention for applications in flexible LIBs. Herein, we first summarize the classification and synthetic methods of emerging 2D noncarbon nanomaterials. The God-given potential and opportunities of these emerging 2D nanomaterials for flexible LIBs are demonstrated along with the features and merits of 2D nanomaterials. Practical applications of 2D nanomaterials as electrode materials for flexible LIBs are reviewed as well. Lastly, this paper summarizes the challenges of flexible LIBs and future prospects of emerging 2D nanomaterials in this promising field.

2. Classification, features and synthetic methods of emerging 2D noncarbon nanomaterials

2.1 Classification

In terms of composition and properties, emerging 2D noncarbon nanomaterials with great prospects for flexible LIBs can be divided into the following four categories: 2D mono-elemental nanomaterials (Xenes), 2D transition metal carbides, nitrides and carbonitrides (MXenes), 2D transition metal dichalcogenides (TMDs) and 2D transition metal oxides (TMOs). Fig. 1 shows the main constituent elements of the four kinds of emerging 2D nanomaterials.

2D mono-elemental nanomaterials such as phosphorene,[82–85] borophene,[86,87] silylene[88] germanene[89] and stanene[90] are categorized as Xenes. With a similar structure to graphene,

Prof. Xiaoling Luo received her PhD from Jinan University in 2004. She is an archiater of Shenzhen People's Hospital. Her major research areas are ophthalmology, fundus disease and biomedical sciences.

Prof. Han Zhang received his BS degree from Wuhan University in 2006 and PhD from Nanyang Technological University in 2010. He is a director of the Shenzhen Key Laboratory of 2D Materials and Devices, and the Shenzhen Engineering Laboratory of Phosphorene and Optoelectronics, Shenzhen University. He is listed in World Highly Cited Researchers (2018). He has published over 260 papers in peer-reviewed journals such as Proceedings of the National Academy of Sciences of the United States of America, Nature Communications, and Laser Photonics Review, with over 40 highly cited papers. His papers have been cited more than 22 000 times (H-index: 75). His current research focus is the synthesis and application of two-dimensional materials for ultrafast and nonlinear photonics, bio-photonics and energy storage.

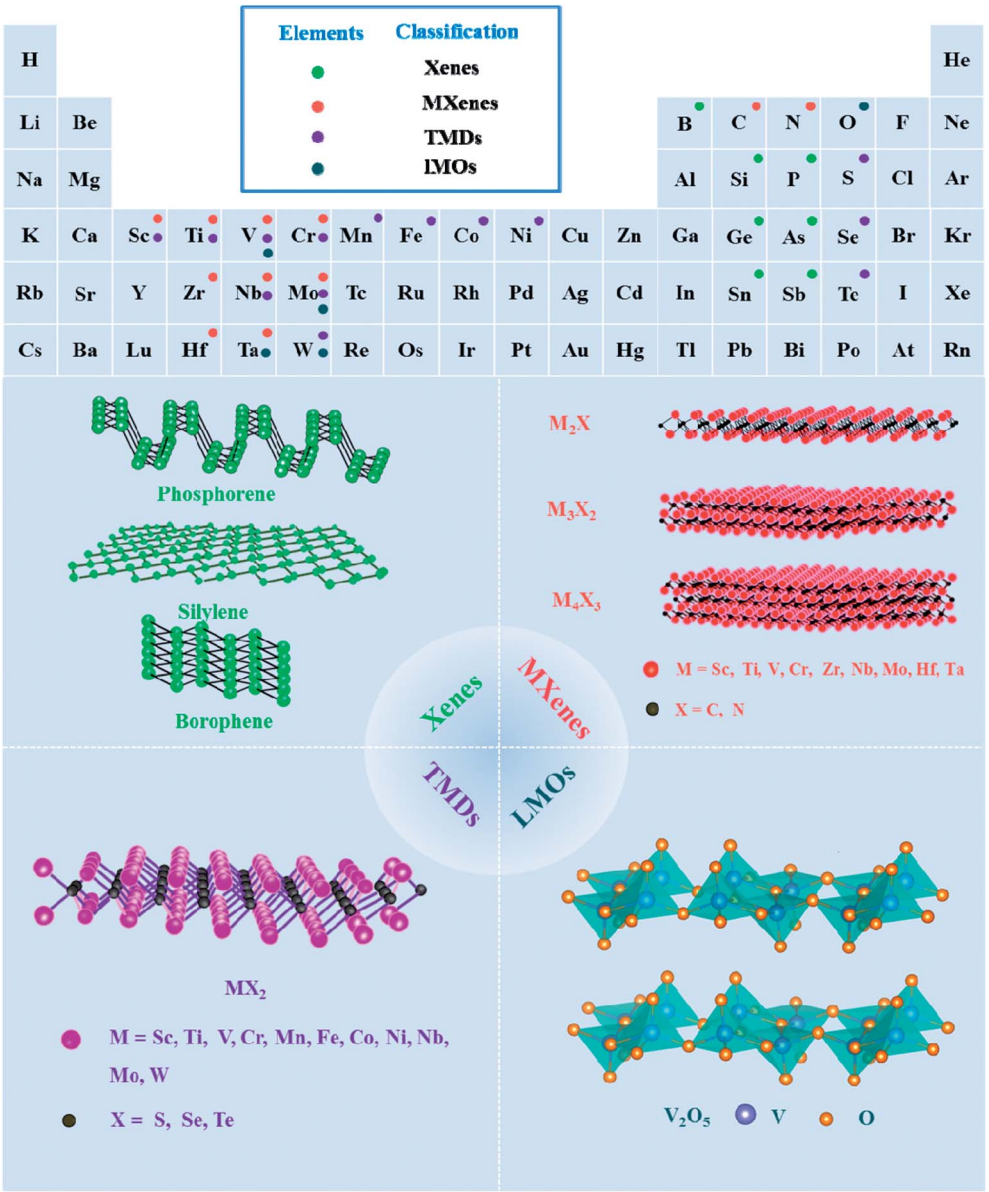

Fig. 1 The main constituent elements of the four kinds of emerging 2D noncarbon nanomaterials and atomic structures of several representative 2D nanomaterials.

these emerging 2D monoelemental nanomaterials have become a research hotspot of new generation advanced materials. The alloying reactions between lithium ions and Xenes can be performed through a multiple electron valence transmission ($M + xLi^+ + xe^- = Li_xM$; M = P, B, Si, Ge, Sn, *etc.*), which is different from the intercalation chemistry of conventional active materials, thus offering great potential for high capacity electrodes.

Another notable family of 2D nanomaterials, layered transition metal carbides, nitrides, and carbonitrides, can be collectively referred to as MXenes.[91–96] MXenes can be synthesized by selective etching of A-group elements (A = Al, Ga, Ti, Si, Ge, Sn, *etc.*) from MAX phases. MAX phases are composed of alternating layers of transition metal elements and A-group elements. MXenes have the general formula of $M_{n+1}X_nT_x$ (n = 1–3), in which M, X, and T symbolize transition metal elements (Sc, Ti, V, Cr, Zr, Nb, *etc.*), carbon or nitrogen elements, and functional groups (–F, –OH, –O, *etc.*), respectively. MXenes exhibit a large layer spacing, good conductivity, low diffusion barrier and outstanding lithium storage capability, showing their potential as electrode materials in LIBs.

TMDs have recently been reported as promising anode candidates for LIBs.[97–100] The general formula of TMDs is MX_2, where M stands for transition metal elements (M = Mo, W, Ti, Zr, V, *etc.*), and X represents chalcogens (X = S, Se, and Te). Similar to MXenes, the layered structure of MX_2 is composed of alternating layers of transition metal elements and chalcogens, where covalent bonds occupy the predominant position within the layer, and adjacent layers are maintained by van der Waals forces. The weak interaction forces between adjacent layers provide the possibility and feasibility to achieve single-layered

TMDs or multilayered TMDs, showing broad prospects as negative electrodes for LIBs.[101–103]

In addition, layered metal oxides (LMOs), which mainly include metal trioxides (MO_3, M = Mo, Ta, W, *etc.*)[104–106] and V_2O_5,[107,108] have also been studied for flexible energy storage applications due to their 2D layered structure, good energy storage properties and superior mechanical properties.

2.2 Features and merits

Towards electrode materials, electrochemical properties and mechanical properties are two crucial factors essentially determining the feasibility for flexible LIBs. Ideal electrode materials should have superior lithium storage capacity, excellent electrical conductivity, and intriguing flexibility. These emerging 2D nanomaterials hold great potential for flexible electrodes because of their favorable properties including unique 2D structure, high specific surface area, good electrochemical activity, ultrahigh lithium storage capacity, and intrinsic flexibility. In this section; emphasis will be focused on the features and merits of emerging 2D nanomaterials for flexible electrodes from these aspects. Table 1 aggregates the relevant property data of several representative emerging 2D noncarbon nanomaterials for LIB electrodes.

Unique crystal structure. The atomic structures of phosphorene, borophene and silicene are illustrated in Fig. 1. As the most stable allotrope of phosphorene, single-layer or few-layer BP consists of a single puckered P atom layer or few puckered P atom layers. Borophene has been reported as an emerging 2D nanomaterial with a periodic corrugation structure. Similarly, silicene, germanene and stanene have been predicted as atomically thick materials with buckled hexagonal honeycomb structures. The atomic structures of M_2X, M_3X_2 and M_4X_3 in Fig. 1 show that $n + 1$ layers of transition metal elements cover n layers of carbon or nitrogen elements in MXenes. The most common structural phases of TMDs are the 2H phase and 1T phase, in which chalcogen atoms are arranged in a trigonal prismatic coordination and octahedral coordination of transition metal atoms, respectively. As for the most widely studied and used TMDs (MX_2: M = Mo or W; X = S, Se or Te), 2H-MX_2 has high thermodynamic stability. The atomic structure of 2H-MX_2 indicates that the M atomic layer is sandwiched by two X atomic layers. Likewise, the crystal structure of α-V_2O_5 in Fig. 1 shows the 2D and layered structure, in which each layer consists of distorted trigonal bipyramidal polyhedra, and the polyhedra share their edges by forming $(V_2O_4)_n$ zigzag double chains along the (001) direction and share their corners by cross-linking along (100).[130,131]

With such unique graphene-like periodic structure, these emerging 2D nanomaterials show many merits including high mechanical strength, high specific surface area, wide diffusion channels and short diffusion length that may contribute to the insertion and extraction of lithium.

Ultrahigh lithium storage capacity. As analogues of graphene, emerging 2D nanomaterials have unique crystal structures with wide interlayer distances. The interlayer spacing and theoretical capacity of several representative emerging 2D nanomaterials are listed in Table 1. 2D nanomaterials have higher interlayer spacings than that of the traditional graphite anode (0.34 nm). The large space in the crystal structure benefits the storage of lithium ions and the larger interlayer distances provide larger channels for the intercalation and de-intercalation of Li-ions, thus facilitating faster Li-ion diffusion. Fig. 2 shows the migration paths for Li diffusion and the lithiated structure of these 2D nanomaterials. As shown in Fig. 2a, BP possesses a puckered structure and provides a 2D channel for the taking off and embedding of lithium ions.[112] Park and Sohn[132] first evaluated BP as an anode material for LIBs, and the result indicated that the reactions of BP with lithium ions in the first discharge process can be expressed as follows: BP → Li_xP → LiP → Li_2P → Li_3P. This illustrated that the fully lithiated phase of BP was Li_3P, and each P atom can combine up to three lithium ions, corresponding to an ultrahigh theoretical specific capacity (2596 mA h g^{-1}), which was sevenfold that of graphite (372 mA h g^{-1}) when used as an anode material for LIBs. Borophene has a planar anisotropic structure and a puckered morphology, which is beneficial to the storage of metal ions. Zhao *et al.*[116] investigated the Li storage capability of borophene, and the calculation results proved that the fully discharged state of borophene is $Li_{0.75}B$, giving it a high theoretical specific capacity of 1860 mA h g^{-1} (Fig. 2b). Mortazavi *et al.*[117] assessed the application prospects of silicene, germanene and stanene as anode materials for LIBs *via* DFT calculations. Fig. 2c shows the structures of lithiated silicene and stanene absorbed with different concentrations of lithium. Calculations predicted that the lithium storage capacities of single-layer silicene, germanene and stanene were 954 mA h g^{-1}, 369 mA h g^{-1} and 226 mA h g^{-1}, respectively.

Table 1 Interlayer spacing, theoretical capacity, and electron mobility of emerging 2D noncarbon nanomaterials

2D nanomaterials	Interlayer spacing (nm)	Theoretical capacity (mA h g^{-1})	Electron mobility (cm^2 V^{-1} s^{-1})
Phosphorene	0.53 (ref. 109–111)	2596 (ref. 112)	~1000 (ref. 113 and 114)
Borophene	0.48 (ref. 115)	1860 (ref. 116)	—
Silicene	—	954 (ref. 117)	1200 (ref. 118)
$Ti_3C_2T_x$	0.99–1.84 (ref. 119)	320 (ref. 92)	2.6 ± 0.7 (ref. 120)
MoS_2	0.62–0.94 (ref. 121)	1290 (ref. 122)	200–1000 (ref. 123 and 124)
WS_2	0.85–1.02 (ref. 125)	433 (ref. 126)	1103 (ref. 127)
V_2O_5	1.15 (ref. 108)	294 (ref. 128)	1.26 (ref. 129)

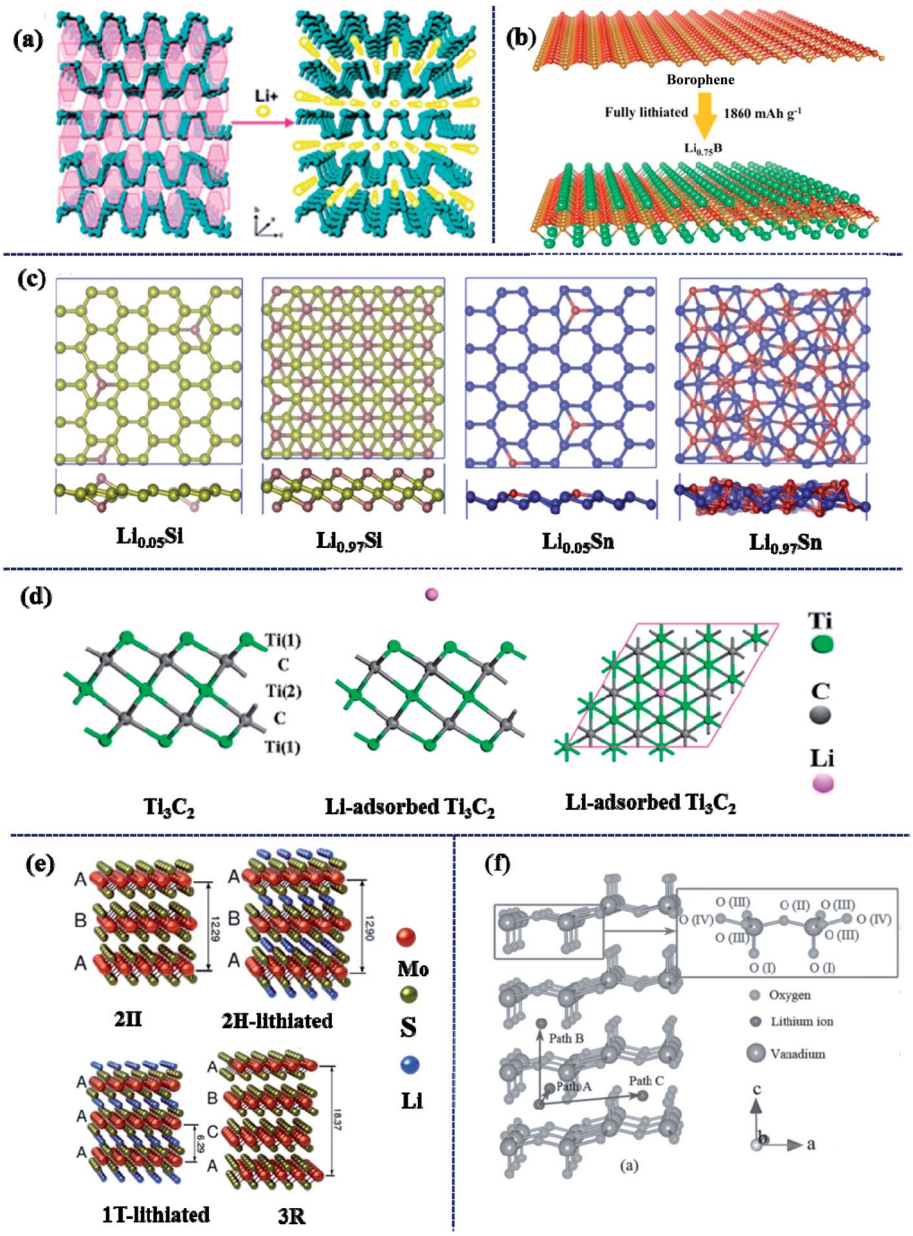

Fig. 2 (a) The crystal structure and transport channels of Li ions of black phosphorus. Reproduced with permission from ref. 112. Copyright 2012, American Chemical Society. (b) Structure of the fully lithiated phase $Li_{0.75}B$. Reproduced with permission from ref. 116. Copyright 2016, Elsevier. (c) Structures of lithiated silicene and stanene. Reproduced with permission from ref. 117. Copyright 2016, Elsevier. (d) Structures of Ti_3C_2 and Li-adsorbed Ti_3C_2. Reproduced with permission from ref. 133. Copyright 2012, American Chemical Society. (e) Molecular models of 2H-MoS_2, lithiated 2H-MoS_2, lithiated 1T-MoS_2, 3R-MoS_2 and Li_2S. Reproduced with permission from ref. 122. Copyright 2014, The Royal Society of Chemistry. (f) Schematic diagram illustrating the crystal structure of V_2O_5 and potential Li^+ diffusion paths. Reproduced with permission from ref. 134. Copyright 2015, John Wiley and Sons.

Tang *et al.*[133] reported the electronic properties of $Ti_3C_2T_x$ and investigated its potential as an anode material for LIBs through DFT computations. The structures of Ti_3C_2 and Li-adsorbed Ti_3C_2 are displayed in Fig. 2d, and the results demonstrated that the single-layer $Ti_3C_2T_x$ with a low Li diffusion barrier and high theoretical capacity could be applied as an active material for LIBs. Fig. 2e shows the idealized molecular models of MoS_2 in structural polytypes, as well as their lithiated counterparts.[122] MoS_2 delivered a high specific capacity (up to 1290 mA h g^{-1}), and this makes MoS_2 a potential negative material for LIBs. The theoretical capacity of V_2O_5 is 294 mA h g^{-1} for two Li^+ insertions. As shown in Fig. 2f, Chu *et al.*[134] discussed three potential paths for Li^+ diffusion in V_2O_5, and it occurred more easily in path A and path C due to its layered structure. On the basis of these research studies above, these emerging 2D nanomaterials with unique crystal structures exhibit ultrahigh lithium storage capacities, which are much higher than that of graphite, showing a large market potential and a bright future as anode materials for LIBs.

High electron mobility and electrical conductivity. Electrochemical reactivity is a crucial factor for assessing the application foreground of LIB electrode materials. 2D nanomaterials, especially monolayer or few-layer ultrathin nanomaterials, have shown high electron mobility and electrical conductivity, ensuring the required electrochemical reactivity when used as anode materials for LIBs. This can be mainly attributed to their extremely high specific surface area, wide layer distance, short diffusion length and plentiful voids and defects.[123,135–137] Particularly, having good electron mobility is essential for active materials, and plenty of research studies show that emerging 2D materials allow achieving these features. Electron mobilities of the 2D nanomaterials are presented in Table 1. In the case of phosphorene, previous research studies have reported that few-layer BP showed a high mobility of ~1000 $cm^2 V^{-1} s^{-1}$.[113,114] Zeng *et al.*[138] studied LIBs assembled with a BP anode electrode *via* the first-principles ultrasoft pseudopotential method. The results indicated that the BP electrode exhibited good conductivity, offering the ability for rapid charging and discharging. Another computational investigation obtained the channel mobilities of single-layer silicene and MoS_2 as 1200 $cm^2 V^{-1} s^{-1}$ and 320 $cm^2 V^{-1} s^{-1}$, respectively.[118] Gogotsi and Sinitskii[120] investigated the electronic properties of $Ti_3C_2T_x$. The field-effect electron mobility of monolayer $Ti_3C_2T_x$ was approximately 2.6 $cm^2 V^{-1} s^{-1}$ and the corresponding conductivity was as high as 4600 S cm^{-1}. The excellent electron transport ability and high intrinsic conductivity of these emerging 2D nanomaterials would greatly enhance the reactivity of the electrochemical reaction, and are conducive to the rapid charge and discharge ability and long cycle life of batteries.

Intrinsic flexibility. The most attractive features of emerging 2D nanomaterials for flexible electrodes is their super intrinsic flexibility. The intrinsic flexibility of 2D nanomaterials has also been verified by many theoretical analyses and experimental studies. For the sake of the intuitive comparison of mechanical properties, the obtained calculation data including ideal strength, Young's modulus and critical strain of emerging 2D nanomaterials are listed in Table 2. According to the unique 2D puckered structure, the mechanical properties of phosphorene are anisotropic. Wei and Peng[139] investigated the mechanical properties of phosphorene by DFT calculations. Along the zigzag and armchair directions, the ideal strengths of single-layer phosphorene were 18 GPa and 8 GPa, and phosphorene can persist up to a tensile strain of 27% and 30%, respectively. The Young's modulus was 166 GPa (zigzag) and 44 GPa (armchair), which are much lower than that of monolayer-graphene (1100 GPa).[140] The mechanical properties of borophene were also calculated based on the DFT method.[141] It was found that borophene exhibited an uppermost flexibility when 1/6 concentration of hollow hexagons was introduced. The corresponding borophene possesses an ideal strength of about 16 N m^{-1}. The Young's modulus was 189 N m^{-1} (armchair) and 210 N m^{-1} (zigzag), and the Poisson ratios were 0.15 (armchair) and 0.17 (zigzag). The equivalent ideal strengths and Young's modulus were 34.2/32.1 GPa and 394/438 GPa along the armchair/zigzag directions with an effective thickness of 4.8 Å for the monolayer borophene. In addition, the tensile stress of borophene could be reduced by introducing more hollow hexagons, lattice phase transitions would be induced by tension, and the borophene could withstand a tensile load up to 48 GPa at strains as high as 40%. Roman and Cranford[142] quantified the elastic stiffness (50.44/62.31 N m^{-1} for the armchair/zigzag directions) and ultimate states (ideal strength of 5.85 N m^{-1} and ultimate strain of 18%) of single-layer silicene based on ReaxFF molecular dynamics. Zhang's group[143] investigated the mechanical stability of 2D layered materials by calculating the Young's modulus and critical strains of silicene, germanene and stanene, as shown in Table 2. The revealed mechanical properties will promote potential applications of these 2D nanomaterials in flexible electronics.

The desirable sensitivity and flexibility of MXenes also suggest great applications of large-magnitude-strain engineering. Gogotsi *et al.*[144] studied the mechanical properties of single-layer and two-layer $Ti_3C_2T_x$. Membranes from single-layer and two-layer $Ti_3C_2T_x$ were successfully synthesized, nanoindentation under different stress was tested using atomic force microscopy (AFM), and then force–displacement curves were obtained. The Young's modulus and breaking strength of the single-layer $Ti_3C_2T_x$ membrane were measured to be 333 ± 30 GPa and 17.3 ± 1.6 GPa. Sun *et al.*[145] systematically studied the stress–strain curves of $Ti_{n+1}C_n$ (n = 1–3), and analyzed the corresponding deformation mechanisms under tensile stress in

Table 2 Mechanical properties of emerging 2D noncarbon nanomaterials

2D nanomaterials	Ideal strengths (armchair/zigzag, GPa)	Young's modulus (armchair/zigzag, GPa)	Critical strains (armchair/zigzag)	Ref.
Phosphorene	8/18	44/166	0.3/0.27	139
Borophene	34.2/32.1	394/438	0.125/0.106	141
Silicene	177.6/178.9	—	0.16/0.16	143
Germanene	92.7/90.9	—	0.2/0.2	143
Stanene	62.2/62.2	—	0.21/0.21	143
$Ti_3C_2T_x$	17.3 ± 1.6	333 ± 30	—	144
Ti_2C	—	620/600	0.1/0.18	145
Ti_2CO_2	—	593/540	0.2/0.28	145
MoS_2	25	270 ± 100	0.06–0.11	146
V_2O_5	—	79.4 ± 3.2	—	148

detail. The data of the corresponding mechanical properties are listed in Table 2. The critical strains of Ti_2C were 9.5% and 18% along the armchair and zigzag directions, respectively. The critical strains of Ti_2CO_2 enhanced to 20% and 28% due to the introduction of oxygen functional groups, which indicated that surface functionalization could effectively ameliorate the mechanical flexibility and was beneficial to the applications of flexible energy storage devices.

Numerous recent studies have demonstrated the superior mechanical properties of TMDs with high elastic strains as well as strong resistance to inelastic fracture. Bertolazzi *et al.*[146] measured the stiffness and breaking strength of single-layer MoS_2 through experimental tests. The breaking strength of single-layer MoS_2 was found to be 23 GPa, and the corresponding Young's modulus was 270 GPa along with a fluctuation of 100 GPa. Using a similar technique, Castellanos-Gomez *et al.*[147] researched the mechanical properties of few-layer MoS_2, and the average Young's modulus was 330 GPa along with a fluctuation of 70 GPa. The above research data indicated the ultrahigh strength of 2D TMDs, providing a powerful ability to withstand large elastic deformation, and making them appropriate for the fabrication of flexible products.

Fateh *et al.*[148] reported the mechanical properties of V_2O_5 thin films grown by reactive magnetron sputtering. The V_2O_5 thin film deposited at room temperature exhibited a hardness of 3.2 GPa and Young's modulus of 79.4 GPa. Du *et al.*[149] reported that the Young's modulus of the MoO_3 thin film was 64.6 GPa *via* the nanoindentation technique. These research studies showed that thin 2D LMOs exhibited good mechanical properties.

2.3 Synthetic methods

There are two main categories of synthetic methods for preparing these emerging 2D noncarbon nanomaterials: top-down approaches and bottom-up synthesis. Fig. 3 shows the schematic diagrams of the two kinds of methods.

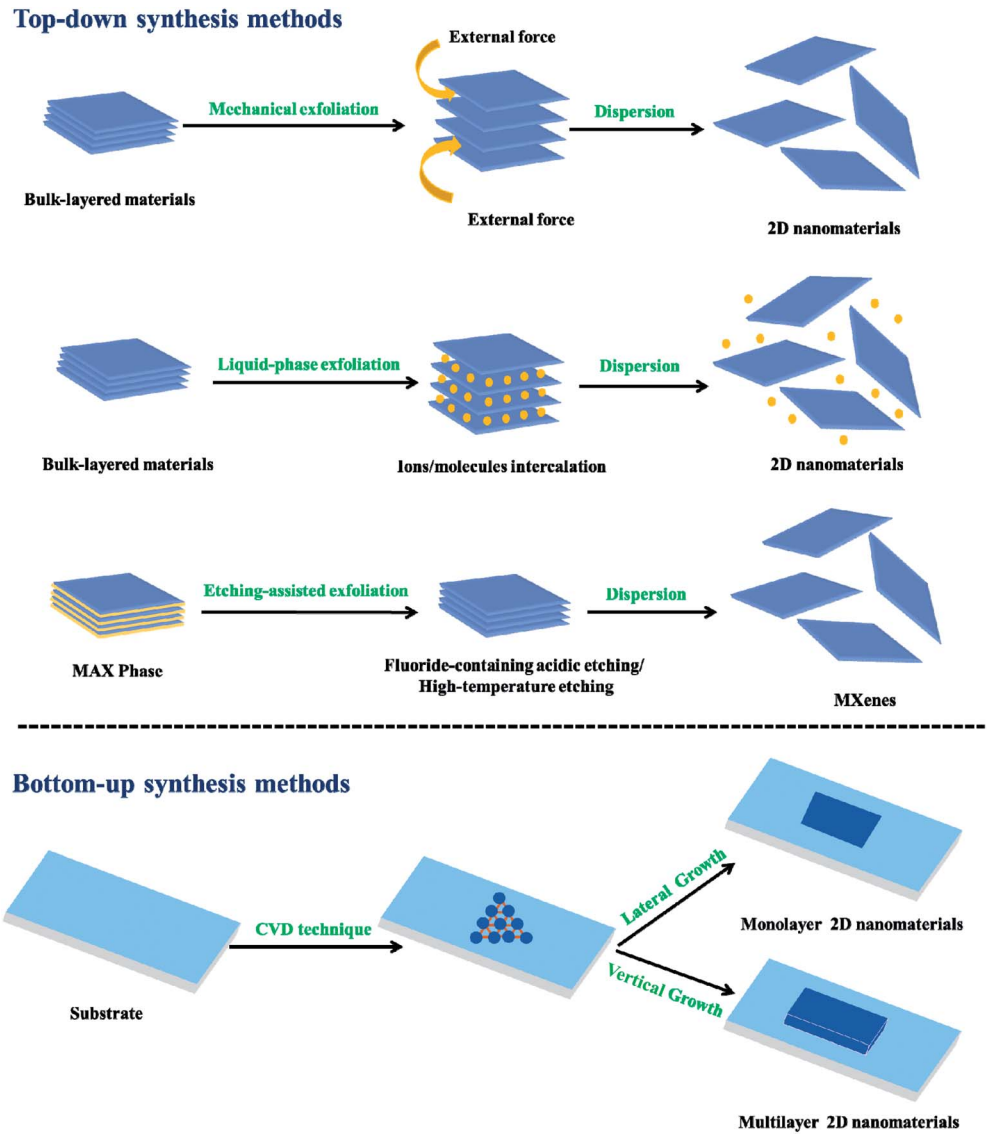

Fig. 3 Schematic diagrams of several common methods to prepare 2D nanomaterials.

Top-down synthesis methods. The most primitive and common synthesis strategy for these 2D nanomaterials is the top-down approach through exfoliating bulk-layered materials to few-layer 2D nanomaterials, mainly including mechanical exfoliation, liquid-phase exfoliation and etching-assisted exfoliation. As shown in Fig. 3, the mechanism of mechanical exfoliation weakens the interactions between the layers of bulk-layered materials with the assistance of the external force through shearing or ball-milling, thus obtaining few-layer 2D nanomaterials. Therefore, mechanical exfoliation is a simple and reliable method without chemical procedures and costly instruments, and the mechanically exfoliated 2D nanomaterials with a clean surface are very appropriate for the basic theoretical study and potential application evaluation. Considerable literature shows that Xenes such as phosphorene, and TMDs such as MoS_2 and WS_2 could be prepared from bulk materials by mechanical exfoliation. For example, many research studies have demonstrated that thin BP flakes can be successfully peeled from bulk crystals *via* a scotch tape-based mechanical exfoliation method.[114,150,151] Likewise, single- and few-layer TMDs (MoS_2, WSe_2, TaS_2, $TaSe_2$, *etc.*) have been exfoliated from bulk materials *via* a scotch tape-based method, and the as-

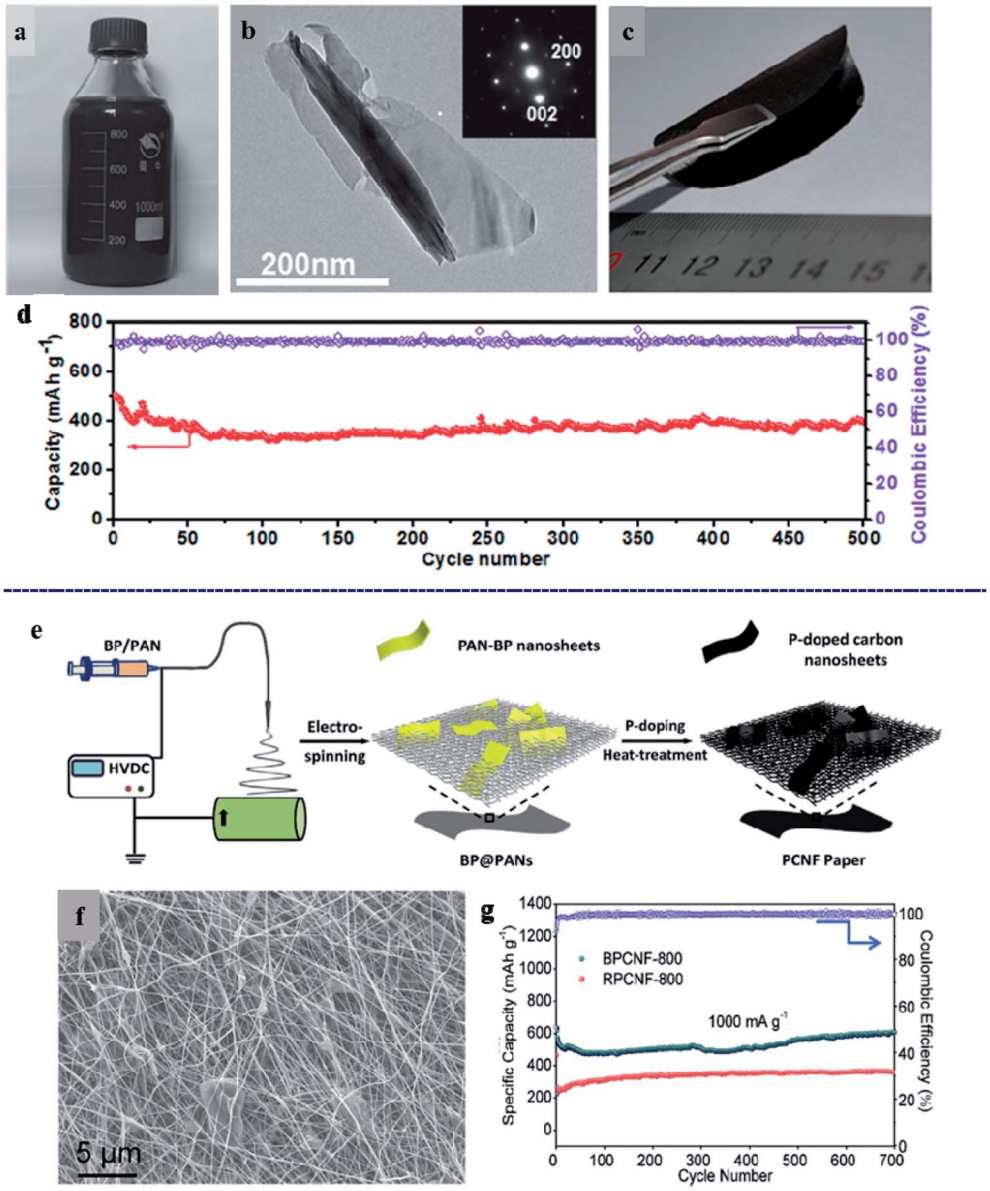

Fig. 4 (a) BP nanosheet dispersion, (b) TEM image of BP nanosheets and the corresponding electron diffraction pattern, (c) photograph of a BP–G hybrid paper with good flexibility and (d) cycling stability and coulombic efficiency of the BP–G hybrid paper electrode. Reproduced with permission from ref. 179. Copyright 2015, John Wiley and Sons. (e) Illustration of the preparation process and (f) SEM image and (g) cycle performance of the flexible phosphorus doped carbon nanosheets/nanofibers. Reproduced with permission from ref. 180. Copyright 2018, Elsevier.

prepared samples exhibited a clean surface and high quality.[152–154] Liu and Komatsu reported the mechanical exfoliation of MoS_2 and WS_2 through the ball-milling reaction, and the obtained 2D nanomaterials could be stored either in the solid state or dispersed in the liquid.[155]

Mechanical exfoliation has the advantages of a short process, simple operation and low cost. However, the method is difficult for scalable production and the mechanically exfoliated 2D nanomaterials may be unstable in the ambient environment.[156,157] Liquid-phase exfoliation is a well-established method for preparing 2D nanomaterials in large quantities.[158] This method for ultrathin 2D nanomaterials is based on expanding the interlayer distance of bulk-layered materials by ion or molecule intercalation (Fig. 4). Liquid-phase exfoliation represents a better option for 2D nanomaterials in terms of high quality and yields, and has been successfully employed for the exfoliation of Xenes, TMDs and LMOs. For instance, 2D BP was realized by liquid phase exfoliation in organic solvents such as *N*-cyclohexyl-2-pyrrolidone (CHP)[158,159] and *N*-methyl-2-pyrrolidone (NMP), and the material size and number of layers were controllable by tuning the exfoliation conditions.[160–162] In addition, many studies reported that MoS_2 nanosheets could be exfoliated from bulk crystals in various kinds of organic solvents.[163,164] LMOs such as 2D a-MoO_3 nanosheets and V_2O_5 nanosheets[165] have been successfully synthesized *via* a simple and scalable liquid-phase exfoliation method.[166,167]

Etching-assisted exfoliation is mainly applied to the synthesis of MXenes by selective etching of A-group atomic layers from the MAX phase. The M–A bond of MAX phases is metallic, and it is difficult to obtain MXenes *via* simple mechanical shearing. The chemical reactivity of M–A bonds is stronger than that of the M–X bonds, providing the possibility for selective etching of A-group atomic layers. The most effective and commonly used etching reagent for the etching-assisted exfoliation of MXenes is a fluoride-containing acidic solution.[168–170] In addition to the acid etching method, MXenes could be prepared *via* high-temperature etching. The Al-layer of the Ti_4AlN_3 precursor could be etched with the help of molten fluoride salts under a high-temperature environment and inert atmosphere, and thus 2D Ti_4N_3 nanomaterials were successfully synthesized.[171]

Bottom-up synthesis methods. Another approach is the bottom-up synthesis method, which mainly includes chemical vapor deposition (CVD) and wet chemical synthesis. 2D nanomaterials can be synthesized in large volumes *via* the bottom-up strategy. CVD has become a widely used method for large area growth of emerging 2D nanomaterials.[172] The schematic diagram of the CVD method for 2D nanomaterial preparation is presented in Fig. 3. The dominant growth direction is controllable under different reaction conditions during the CVD process, and finally the area and layer number of the products are determined. Many 2D nanomaterials have been successfully designed and synthesized through the CVD method. Smith *et al.*[173] proposed an *in situ* CVD method for the large-area growth of few-layer BP. What's more, area-controlled and layer-controlled 2D TMDs[174–176] and 2D LMOs[177,178] have also been achieved by the CVD method.

3. Practical applications in flexible LIBs

Having the advantages of high lithium storage capacity, good electron mobility and electrical conductivity, and intriguing flexibility, the aforementioned 2D nanomaterials have been more and more attractive in materials technology, and have been widely researched and used in flexible LIBs. The following sections summarize the practical applications of 2D nanomaterials as electrode materials for flexible LIBs with choosing phosphorene, $Ti_3C_2T_x$, MoS_2, WS_2 and V_2O_5 as representatives.

3.1 Phosphorene

The layer structures held together by van der Waals forces provide Xenes with an ultra-large specific surface area, wide interlayer distances, electrochemical reactivity and superior mechanical properties. Phosphorene has become an appealing candidate for flexible LIBs with these outstanding properties. Ren *et al.*[179] reported a flexible BP–G hybrid paper which was fabricated with centrifugation-exfoliated BP nanoflakes and intercalation-exfoliated few-layer graphene *via* vacuum filtration. Fig. 4a shows a bottle of BP nanosheet dispersion, and the TEM image in Fig. 4b indicates the ultrathin thickness and smooth surface of BP nanosheets. The photograph of the paper-like BP–G electrode in Fig. 4c demonstrates its good flexibility and bendability. After 500 cycles at 500 mA g^{-1}, the as-prepared flexible electrode still delivered a capacity of 402 mA h g^{-1} with a high capacity retention ratio of 80.2%. The outstanding long life span at large current density demonstrates the great potential of BP nanosheets as the electrode material for flexible LIBs. Xie *et al.*[180] fabricated a free-standing carbon nanofiber paper doped with BP nanosheets *via* electrospinning (Fig. 4e). The as-prepared BP/CNF paper was formed of 3D interconnected nanofibers and BP nanosheets (Fig. 4f). When used as the anode electrode for LIBs, the flexible paper maintained a superior specific capacity of 607 mA h g^{-1} after 700 cycles without obvious decay even at 1000 mA g^{-1} (Fig. 4g).

Recently, several studies embarked on theoretical research of 2D heterostructures assembled from phosphorene and other 2D nanomaterials. For example, Peng *et al.*[181] reported theoretical calculations with respect to heterostructures assembled from blue phosphorene and MS_2 (M = Nb, Ta) for flexible LIBs. The findings showed that BlueP/MS_2 heterostructures would exhibit good stability, good conductivity, large ultimate strains and high Li storage capacity, indicating the rosy prospect of heterostructures for next-generation flexible energy storage devices. Similarly, the BP/TiC_2 heterostructure was theoretically proven to possess high stability, good conductivity, superior flexibility and high theoretical capacity, and become a promising candidate for flexible LIBs.[182]

3.2 MXene

With a remarkable mechanical flexibility and high energy storage capacity, MXenes have been predicted to be applicable in flexible energy storage devices such as LIBs, sodium-ion batteries (SIBs) and supercapacitors. Among various MXene families, the earliest discovered $Ti_3C_2T_x$ family with excellent flexibility and metallic conductivity is the most widely studied and reported, and is widely applied in the field of flexible energy storage. Tang *et al.*[133] performed DFT computations to evaluate Ti_3C_2 as an anode material for LIBs. Attractive properties related to electronic conductivity, ion diffusion and lithium storage would favor the potential applications of Ti_3C_2 for LIBs. Gogotsi *et al.*[183] reported a series of flexible and conductive $Ti_3C_2T_x$-based composite films. The films formed from $Ti_3C_2T_x$ layers with polymer binders or spacers demonstrated superior mechanical flexibility as well as good electrical conductivity, and could even be folded into a paper airplane (Fig. 5a). The remarkable mechanical performance and impressive electrochemical properties provided these $Ti_3C_2T_x$ films with great application value in flexible electronic devices. Afterwards, flexible composite films of $Ti_3C_2T_x$ and transition metal oxides (TMOs) were synthesized by the same group. Binder-free and self-standing $Ti_3C_2T_x$/TMOs films could be achieved *via* an alternating filtration route, spray coating method or *in situ* wet chemistry synthesis. The resulting films showed satisfactory electrochemical performance when used for LIBs (Fig. 5c).[184] Gogotsi *et al.*[185] reported a $Ti_3C_2T_x$/CNTs composite film and

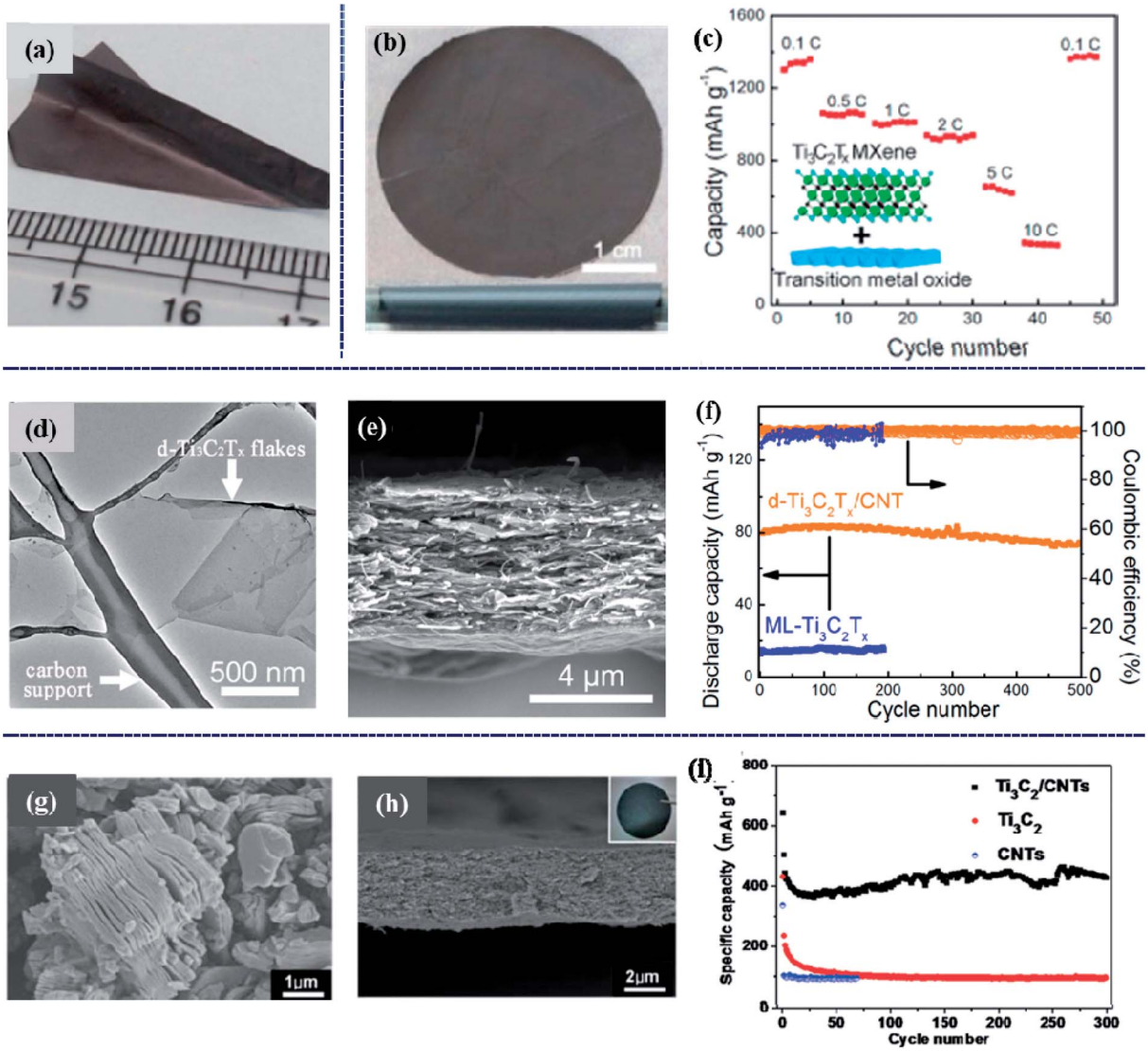

Fig. 5 (a) A $Ti_3C_2T_x$ film was folded into the shape of a paper airplane. Reproduced with permission from ref. 183. Copyright 2014, Proceedings of the National Academy of Sciences. (b) The picture and (c) the rate performance of the free-standing $Ti_3C_2T_x/Co_3O_4$ films. Reproduced with permission from ref. 184. Copyright 2016, Elsevier. (d) TEM image of d-$Ti_3C_2T_x$ flakes, (e) cross-sectional SEM image of d-$Ti_3C_2T_x$/CNT and (f) cycle stability of d-$Ti_3C_2T_x$/CNT cathodes. Reproduced with permission from ref. 185. Copyright 2017, American Chemical Society. (g) SEM image of Ti_3C_2, (h) SEM image of Ti_3C_2/CNTs paper and (i) cycling performance of Ti_3C_2, Ti_3C_2/CNTs and CNTs. Reproduced with permission from ref. 186. Copyright 2015, The Royal Society of Chemistry.

even extended its application to hybrid Mg^{2+}/Li^{+} batteries. d-$Ti_3C_2T_x$ flakes with a graphene-like morphology were produced from Ti_3AlC_2 *via* HF etching (Fig. 5d), and then were used in the formation of a flexible composite film with addition of CNTs (Fig. 5e). Fig. 5f demonstrates the good cycling stability of the $Ti_3C_2T_x$/CNT electrode when used in hybrid Mg^{2+}/Li^{+} batteries.

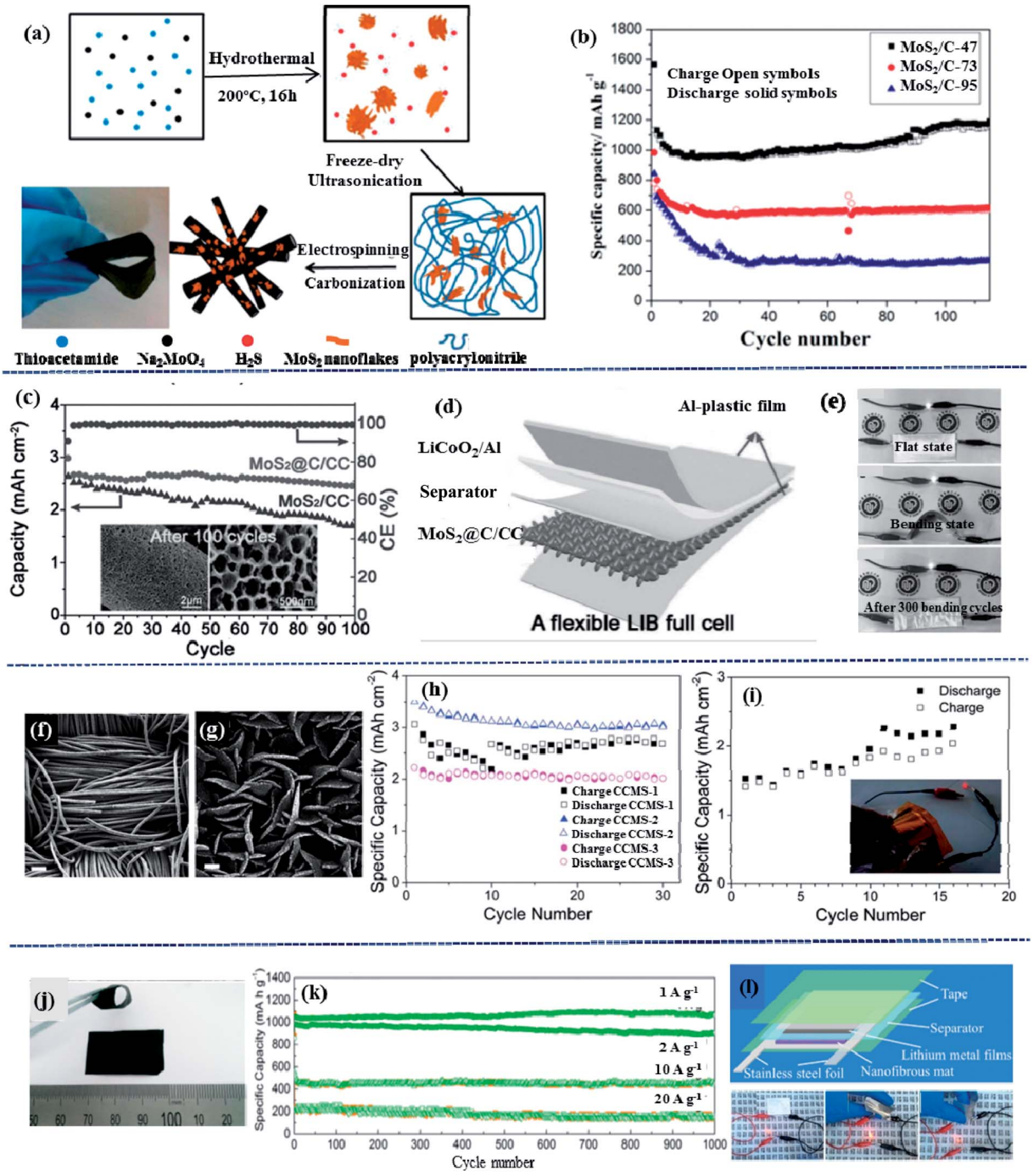

Fig. 6 (a) Schematics of the fabrication process for the highly flexible free-standing MoS_2/C and (b) the cycling performance. Reproduced with permission from ref. 187. Copyright 2014, American Chemical Society. (c) Rate and cycling performance of the coin-type full battery, (d) schematic illustration of a flexible full battery and (e) a white LED lit by the flexible full battery under the flat state, bent state, and even after 300 bending cycles. Reproduced with permission from ref. 188. Copyright 2017, John Wiley and Sons. (f and g) SEM images of 3D hierarchical MoS_2/CC, (h) cycling performance of MoS_2/CC, and (i) the cycling performance of the full battery with the inset showing that the flexible full battery can light a red LED even after 50 cycles of bending the full battery. Reproduced with permission from ref. 189. Copyright 2014, The Royal Society of Chemistry. (j) A photograph of the self-supported flexible C@TiO_2/MoS_2 electrode, (k) cycling performance of the C@TiO_2/MoS_2 electrode and (l) scheme of the flexible battery and a red LED lit by the flexible battery under different states. Reproduced with permission from ref. 190. Copyright 2017, Elsevier.

Peng *et al.*[186] also previously reported the $Ti_3C_2T_x$/CNTs film (Fig. 5e). When used as an anode for LIBs, the $Ti_3C_2T_x$/CNTs film delivered a capacity of 428 mA h g^{-1} at 0.5C after 300 cycles, indicating its excellent cycling performance.

3.3 MoS_2

Owing to their favourable mechanical properties and excellent electrical characteristics, MoS_2 nanosheets become a popular material for the realization of flexible LIBs. Hydrothermally synthesized MoS_2 nanoflakes were encapsulated into amorphous carbon nanofibrous mats, and then were used to fabricate the flexible MoS_2/C film *via* electrospinning and carbonization (Fig. 6a). The MoS_2/C composite film formed with 47% MoS_2 exhibited the best electrochemical performance, delivering a capacity of 1150 mA h g^{-1} after 100 cycles, and the corresponding capacity retention ratio exceeded 100%.[187] Deng *et al.*[188] designed and synthesized a flexible MoS_2@C/CC anode for LIBs. 3D ordered macroporous MoS_2@C nanostructures were prepared *via* a template method with the assistance of polystyrene nanospheres, and then were assembled onto carbon cloth to fabricate the flexible MoS_2@C/CC anode. The as-prepared flexible anode delivered a high capacity of 2.47 mA h cm^{-2} at a current density of 0.5 mA cm^{-2} after 100 cycles, which was much higher than that of the MoS_2/CC electrode (Fig. 6c). A full flexible LIB was successfully fabricated with the schematic illustration shown in Fig. 6d. In order to further evaluate the flexibility, a white LED was connected with the full LIBs under the states of flat, bent and bent after 300 cycles. The brightness of the white LED almost kept unchanged under different states (Fig. 6e). Yu *et al.*[189] reported a 3D hierarchical MoS_2/CC electrode *via* a one-step hydrothermal reaction. The flexible MoS_2/CC electrode delivered a high reversible capacity of 3.0 mA h cm^{-2} at 0.15 mA cm^{-2} after 30 cycles (Fig. 6h). A full flexible LIB was assembled using the MoS_2/CC electrode with a commercial $LiCoO_2$ electrode, and was then characterized by the charge–discharge test and using a commercial red LED. The cycle performance and the picture of the lit red LED in Fig. 6i demonstrated the excellent flexibility and good electrochemical properties of the MoS_2/CC electrode. Wang *et al.*[190] synthesized a self-supporting C@TiO_2/MoS_2 electrode *via* a hydrothermal method. The resulting electrode exhibited extremely excellent electrochemical performance, and it delivered a capacity of 1072 mA h g^{-1} at 1000 mA g^{-1} after 1000 cycles, indicating the remarkable cycle life of the flexible electrode (Fig. 6k). The flexible LIBs were assembled using the C@TiO_2/MoS_2 anode and lithium metal cathode with $LiPF_6$ as the electrolyte, and the resulting flexible LIBs could light the red LED regardless of under the flat state or bent state.

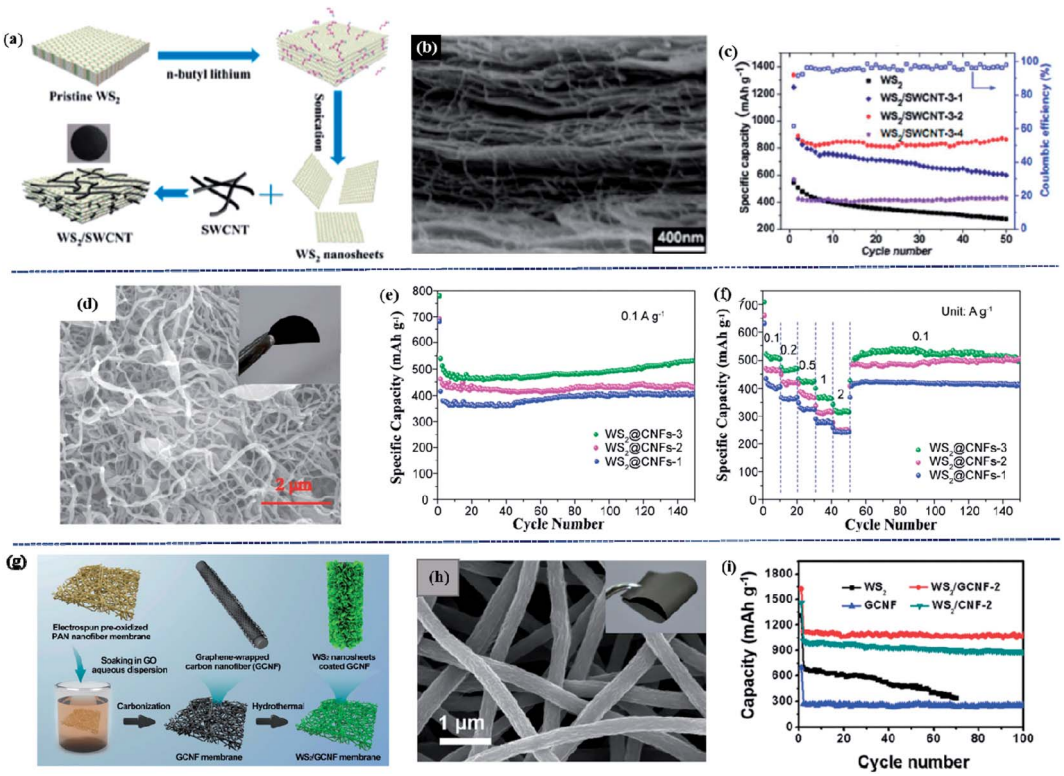

Fig. 7 (a) Schematic of the preparation process of WS_2/SWCNT films, (b) cross-section SEM image of the WS_2/SWCNT film and (c) cycling performance of the flexible films. Reproduced with permission from ref. 191. Copyright 2014, The Royal Society of Chemistry. (d) SEM image of WS_2@CNFs composites with the inset digital photograph showing a folded WS_2@CNF membrane electrode, (e) cycling performance and (f) rate capability of WS_2@CNFs electrodes. Reproduced with permission from ref. 192. Copyright 2017, John Wiley and Sons. (g) Schematic of the preparation of the flexible WS_2/GCNF film, (h) SEM image of the WS_2/GCNF film and (i) cycle performance of the WS_2/GCNF electrode. Reproduced with permission from ref. 193. Copyright 2016, The Royal Society of Chemistry.

3.4 WS_2

As another typical TMD, WS_2 has gained tremendous attention as an anode material for LIBs due to its high theoretical specific capacity (433 mA h g^{-1}). Just like MoS_2, WS_2 nanosheets assembled with conductive carbon-based materials have been widely applied as active materials for flexible LIBs. As shown in Fig. 7a, the WS_2/SWCNT composite film could be synthesized *via* a simple vacuum filtration route. SWCNTs and WS_2 nanosheets were uniformly mixed to obtain a composite film with a porous network structure (Fig. 7b)[191] The as-prepared WS_2/SWCNT exhibited the highest cycling stability when the mass ratio of WS_2 to SWCNT was 3 : 2 (Fig. 7c). After 50 cycles at 100 mA g^{-1}, the discharge capacity of the films was maintained at 861 mA h g^{-1}. Wei *et al.*[192] reported a flexible WS_2@CNF membrane electrode prepared by hydrothermal synthesis and electrospinning. The resulting WS_2@CNFs film exhibited a porous morphology (Fig. 7d), and displayed a discharge specific capacity of 545 mA h g^{-1} at a current density of 500 mA g^{-1} after 800 cycles (Fig. 7e). In addition to excellent cycling performance, the as-prepared WS_2@CNF electrode showed superior rate performance, retaining a good discharge capacity (62.4% of that at 100 mA g^{-1}) at 2000 mA g^{-1}, and cycled stably when the current density was back to 100 mA g^{-1} (Fig. 7f). Zhang *et al.*[193] proposed a novel method to prepare a flexible WS_2/GCNF film for LIBs, and the corresponding schematic of the preparation process is shown in Fig. 7g. The flexible WS_2/GCNF electrode delivered a charge capacity of 1069 mA h g^{-1} at 100 mA g^{-1} after 100 cycles, and the corresponding capacity retention was as high as 95% (Fig. 7i).

3.5 V_2O_5

With a layered crystal structure and good flexibility, 2D V_2O_5 is believed to be a potential candidate for the flexible LIB electrode material. Zhi *et al.*[194] reported a self-supported flexible V_2O_5@G electrode through encapsulating V_2O_5 into carbon nanotubes, as shown in Fig. 8. After 200 cycles at a current density of 150 mA g^{-1}, the V_2O_5@G electrode still maintained a capacity of 211 mA h g^{-1}, demonstrating 91.7% capacity retention. Nicolosi's group[165] produced a flexible and binder-free V_2O_5 NS/SWCNT hybrid electrode *via* ultrasonic aerosol printing. The resulting flexible composite electrode also exhibited high capacities and good cycling performance (Fig. 8h).

Table 3 summarizes the cycling performance of emerging 2D noncarbon nanomaterials when applied to flexible LIBs. Compared with the flexible electrode formed using a flexible substrate and traditional active materials, most of the flexible electrodes formed using emerging 2D noncarbon nanomaterials demonstrated superior lithium storage properties

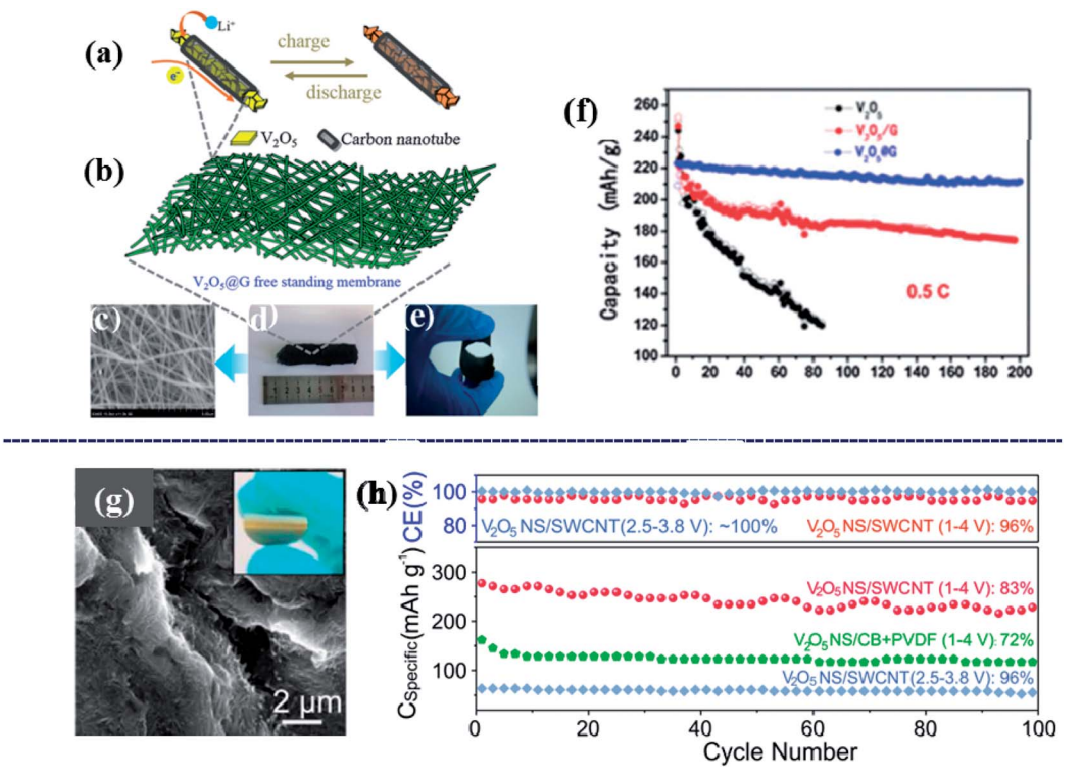

Fig. 8 (a) Schematic diagram of a graphitic nanotube encapsulated with a V_2O_5 nanosheet, (b) schematic of the configuration of the self-supported flexible V_2O_5@G membrane interwoven by nanocables, (c) SEM images of the V_2O_5@G membrane, (d and e) photographs of the self-supported flexible V_2O_5@G membrane under flat and bent states, and (f) different cycle performances of V_2O_5@G, V_2O_5/G and pure V_2O_5 electrodes at a current density of 0.5C. Reproduced with permission from ref. 194. Copyright 2016, The Royal Society of Chemistry. (g) SEM image and photograph of the flexible V_2O_5 NS/SWCNT electrode and (h) cycling performance and coulombic efficiency of V_2O_5 NS and V_2O_5 NS/SWCNT electrodes. Reproduced with permission from ref. 165. Copyright 2017, Elsevier.

Table 3 Summary of cycling performance of emerging 2D noncarbon nanomaterials for flexible LIBs

Electrodes	Cycle number	Current density	Specific capacity	Capacity retention ratio	Ref.
BP/G	500	500 mA g^{-1}	402 mA h g^{-1}	80.2%	179
BP/CNF	700	1000 mA g^{-1}	607 mA h g^{-1}	—	180
Ti_3C_2/CNTs	300	0.5C	428 mA h g^{-1}	—	186
MoS_2/C	100	50 mA g^{-1}	1150 mA h g^{-1}	101.5%	187
MoS_2@C/CC	100	0.5 mA cm^{-2}	2.47 mA h cm^{-2}	93%	188
MoS_2/CC	30	0.15 mA cm^{-2}	3 mAh cm^{-2}	85.7%	189
C@TiO_2/MoS_2	1000	1000 mA g^{-1}	1072 mA h g^{-1}	>100%	190
WS_2/SWCNT	50	100 mA g^{-1}	861 mA h g^{-1}	97%	191
WS_2@CNFs	800	500 mA g^{-1}	545 mA h g^{-1}	>93%	192
WS_2/GCNF	100	100 mA g^{-1}	1068.5 mA h g^{-1}	95%	193
V_2O_5@G	200	150 mA g^{-1}	211 mA h g^{-1}	91.7%	194
V_2O_5/SWCNT	100	1C	—	83%	165

and excellent cycling stability. What's more, the intrinsic flexibility and good membrane-forming properties of these 2D nanomaterials could guarantee the mechanical properties and structural stability of the self-supported flexible electrodes. The outstanding lithium storage properties and flexibility would attract more attention to the research of these emerging 2D nanomaterials, and provide great potential for their applications in flexible LIBs.

4. Challenges and future prospects

The great market prospects and rapid developments of flexible electronic products, wearable medical devices and wearable sports products have created an urgent demand for flexible energy storage devices. Flexible LIBs show great application potential in the field of flexible energy storage devices due to their unique advantages such as light weight, high power and energy density, and long cycling life. The intrinsic rigidity of traditional active materials cannot meet the requirement of high mechanical strength for flexible LIBs. Endowing traditional active materials with flexibility through a flexible matrix will significantly limit the flexibility of the electrode and reduce the energy density of the whole flexible device. Therefore, the fabrication of flexible LIBs possessing both superior mechanical properties and excellent electrochemical performances seems like a formidable challenge. Recently, many emerging 2D nanomaterials including Xenes, MXenes, TMDs and LMOs have shown great potential as active materials for flexible LIBs due to their rapid mobility, high surface area, large interlayer spacing and adjustable electronic properties. The wide interlayer spacing, huge specific surface area and plentiful defects of 2D nanomaterials provide large diffusion channels and many active sites for lithium ions, favoring the storage of lithium ions and the rapid lithiation/delithiation process. In addition, the remarkable mechanical strength and flexibility of 2D nanomaterials offer new prospects for flexible energy storage devices.

Although 2D nanomaterials have shown a tremendous application foreground in flexible energy storage devices because of their unique structures and electronic properties, the practical application in flexible LIBs is still an emerging field full of difficulties and challenges. The main challenges and future prospects mainly include the following aspects:

(1) Large-scale and mass production of 2D nanomaterials with high efficiency and low cost remains a challenge. The synthesis procedure plays an important role in the electrochemical performance of 2D nanomaterials, arduous layer-by-layer exfoliation is the most frequently used and simple preparation strategie for these emerging 2D nanomaterials. The low yield and complex process seriously restrict the practical application, and are not suitable for several particular 2D nanomaterials. For example, silicene cannot be exfoliated from bulk crystals because it is too difficult to break the sp^3-hybridized Si–Si bonds in the bulk silicon. In practice, a new realizable method for fabricating silicene and borophene is molecular beam epitaxy (MBE), which is based on the epitaxial growth of silicon or boron atoms on the Ag(111) surface.[124,195] Therefore, more neoteric methods should be developed to enhance productivity, reduce production cost and realize the preparation of some particular 2D nanomaterials.

(2) New 2D nanomaterials and novel 2D constructions should be developed for further excavating and utilizing the superiority of 2D nanomaterials for flexible LIBs. Considering the unique properties of individual 2D nanomaterials, as well as a similar structure between two components, structural design and practical synthesis of 2D heterojunctions becomes a feasible method for the development and applications of new 2D nanomaterials.[196–201] Graphene/TMD heterostructures such as graphene/MoS_2,[202] TMDs/TMD heterostructures such as WS_2/MoS_2 (ref. 203) and MoS_2/$MoSe_2$,[204] and TMDCs/h-BN heterostructures such as MoS_2/h-BN[205] have been resoundingly grown *via* the CVD technique. Monolayer atomic crystal molecular superlattices are another kind of most prospective 2D construction.[206] Duan *et al.*[207] designed and synthesized several novel stable superlattices *via* an electrochemical molecular intercalation approach. The results showed that the superlattices were composed of alternating monolayer atomic crystals with molecular layers. The as-prepared monolayer phosphorene molecular superlattices (MPMS) exhibited a large interlayer distance over twice that of black phosphorus. This study provides an efficient strategy to synthesize 2D superlattices, and

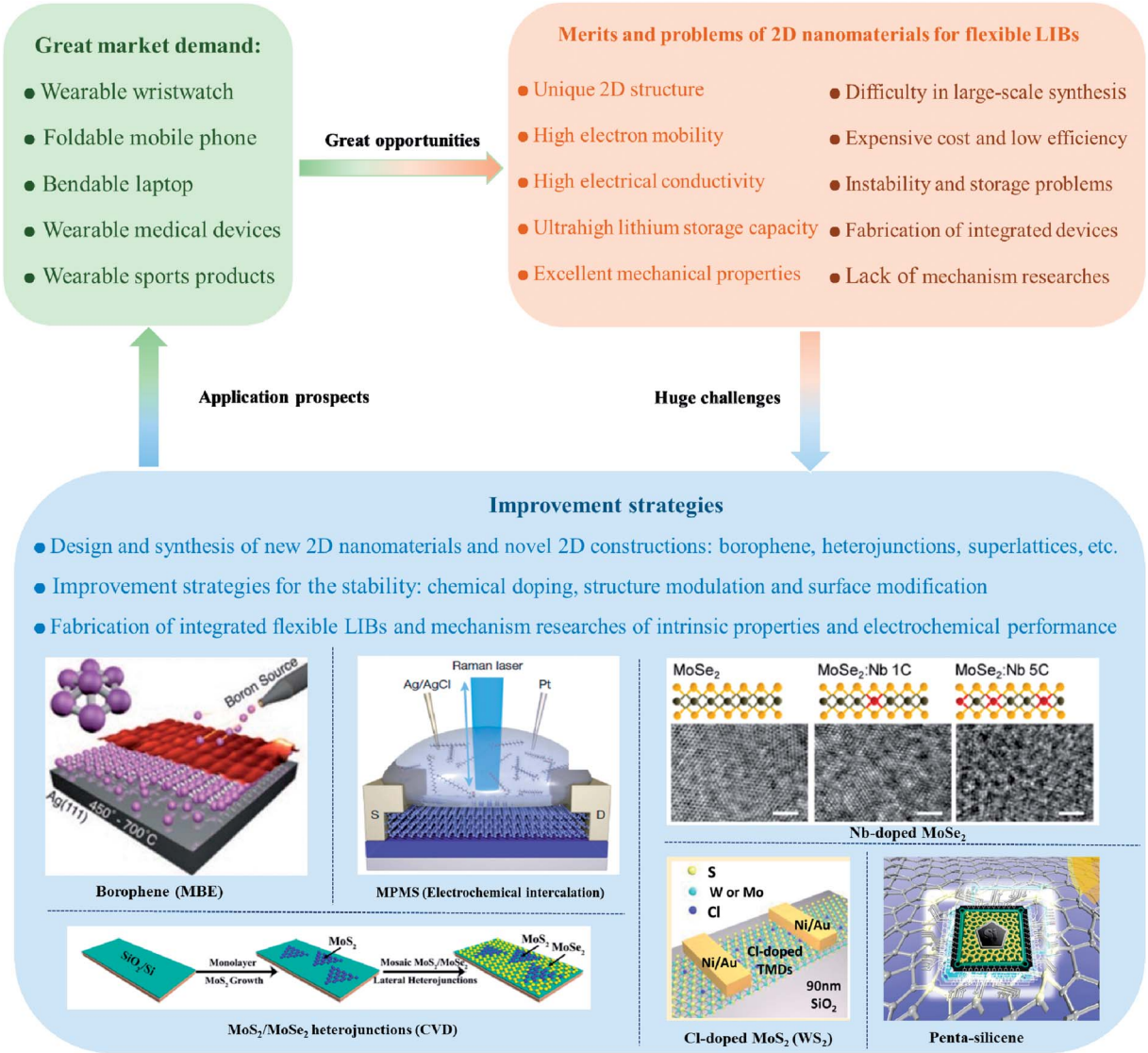

Fig. 9 Opportunities, challenges and future prospects of emerging noncarbon 2D nanomaterials for flexible LIBs.[99,195,204,207,211,212] Reproduced with permission from ref. 99. Copyright 2018, American Association for the Advancement of Science; reproduced with permission from ref. 195. Copyright 2018, Springer Nature; reproduced with permission from ref. 204. Copyright 2017, American Chemical Society; reproduced with permission from ref. 207. Copyright 2017, American Chemical Society; reproduced with permission from ref. 211. Copyright 2014, American Chemical Society; reproduced with permission from ref. 212. Copyright 2019, The Royal Society of Chemistry.

more innovative strategies should be promoted to explore new 2D nanomaterials and novel 2D constructions with desirable electrochemical and mechanical properties, thus offering greater advantages for flexible LIBs.

(3) The abundant defects in newly produced 2D nanomaterials will lead to low physicochemical stability, while the stability is a crucial factor to evaluate the practicability of 2D nanomaterials. 2D nanomaterials have unique properties and extraordinary engineering applications. However, the properties of 2D nanomaterials are easy to become unstable over time. Fortunately, 2D nanomaterials have an extremely large specific surface area, providing abundant surface atoms and surface sites and therefore provide a way to modify surface structures for efficiently engineering their intrinsic properties. Strategies such as chemical doping, structural modulation and surface modification, which influence the intrinsic properties without destroying the pristine 2D structures are vital for developing 2D nanomaterials in flexible devices.[208–210] For example, research has shown that the stability of $MoSe_2$ and MoS_2 was improved with suitable Nb dopants and Cl dopants, respectively.[99,211] Chen *et al.*[212] recently reported that unstable penta-silicene could be turned into new stable 2D nanomaterials after surface chemistry reconfiguration based on first-principles calculations. The functionalized penta-silicene demonstrated high stability, superior mechanical properties and excellent electronic properties, indicating its applied feasibility and prospects for application as an anode material for flexible LIBs.

(4) Until now, most research is limited to the battery-level performance of a single flexible electrode, and the related mechanism research still remains preliminary. Therefore, the fabrication of integrated flexible LIBs and in-depth research are required to reveal the interaction mechanism of the intrinsic properties and electrochemical performance of 2D nanomaterials, and provide a theoretical foundation for practical application of flexible energy storage devices (Fig. 9).

Conflicts of interest

There are no conflicts to declare.

Acknowledgements

The research was partially supported by the National Natural Science Fund (Grant No. 61875138, 61435010, and 6181101252), and Science and Technology Innovation Commission of Shenzhen (KQTD2015032416270385, JCYJ20150625103619275, and JCYJ20170811093453105). The authors also acknowledge the support from the Instrumental Analysis Center of Shenzhen University (Xili Campus).

References

1 C. Agnès, M. Holzinger, A. L. Goff, B. Reuillard, K. Elouarzaki, S. Tingry and S. Cosnier, *Energy Environ. Sci.*, 2014, **7**, 1884–1888.
2 M. G. Kim and J. Cho, *Adv. Funct. Mater.*, 2010, **19**, 1497–1514.
3 A. Manthiram, A. V. Murugan, A. Sarkar and T. Muraliganth, *Energy Environ. Sci.*, 2008, **1**, 621–638.
4 Y. Liu, K. He, G. Chen, R. L. Wan and X. Chen, *Chem. Rev.*, 2017, **117**, 12893.
5 L. Li, Z. Wu, S. Yuan and X. B. Zhang, *Energy Environ. Sci.*, 2014, **7**, 2101–2122.
6 H. F. Ju, W. L. Song and L. Z. Fan, *J. Mater. Chem. A*, 2014, **2**, 10895–10903.
7 X. Chen, J. A. Rogers, S. P. Lacour, W. Hu and D.-H. Kim, *Chem. Soc. Rev.*, 2019, **48**, 1431–1433.
8 A. M. Abdelkader, N. Karim, C. Vallés, S. Afroj, K. S. Novoselov and S. G. Yeates, *2D Mater.*, 2017, **4**, 035016.
9 S. Ding, D. Zhang, J. S. Chen and X. W. Lou, *Nanoscale*, 2011, **4**, 95–98.
10 I. Mukhopadhyay, N. Hoshino, S. Kawasaki, F. Okino, W. K. Hsu and H. Touhara, *ChemInform*, 2010, **33**, A39–A44.
11 J. Qian, W. A. Henderson, W. Xu, P. Bhattacharya, M. Engelhard, O. Borodin and J. G. Zhang, *Nat. Commun.*, 2015, **6**, 6362.
12 V. Strong, S. Dubin, M. F. Elkady, A. Lech, Y. Wang, B. H. Weiller and R. B. Kaner, *ACS Nano*, 2012, **6**, 1395–1403.
13 R. Wang, X. Li, Z. Wang and Z. Han, *Nano Energy*, 2017, **34**, 131–140.
14 C. Yuan, H. B. Wu, Y. Xie and X. W. Lou, *Angew. Chem., Int. Ed.*, 2014, **53**, 1488–1504.
15 Z. Zhu and X. Chen, *Nano Res.*, 2017, **10**, 4138.
16 Y. He, B. Matthews, J. Wang and L. Song, *J. Mater. Chem. A*, 2016, **6**, 735–753.
17 Y. Hu and X. Sun, *ChemInform*, 2014, **2**, 10712–10738.
18 G. M. Zhou, F. Li and H. M. Cheng, *Energy Environ. Sci.*, 2014, **7**, 1307–1338.
19 J. Chen, Y. Liu, A. I. Minett and C. Crean, *Chem. Mater.*, 2007, **19**, 3595–3597.
20 Z. Gao, N. Song, Y. Zhang and X. Li, *Nano Lett.*, 2015, **15**, 8194–8203.
21 Z. Huang, Z. Zhang, X. Qi, X. Ren, G. Xu, P. Wan, X. Sun and H. Zhang, *Nanoscale*, 2016, **8**, 13273.
22 C. Y. Wang, A. M. Ballantyne, S. B. Hall, C. O. Too, D. L. Officer and G. G. Wallace, *J. Power Sources*, 2006, **152**, 610–614.
23 J. Z. Wang, S. L. Chou, J. Chen, S. Y. Chew, G. X. Wang, K. Konstantinov, J. Wu, S.-X. Dou and H. K. Liu, *Electrochem. Commun.*, 2008, **10**, 1781–1784.
24 Z. Zhen, Y. Liu, R. Long, Z. Han, Z. Huang, Q. Xiang, X. Wei and J. Zhong, *Electrochim. Acta*, 2016, **200**, 142–151.
25 S. L. Chou, J. Z. Wang, S. Y. Chew, H. K. Liu and S. X. Dou, *Electrochem. Commun.*, 2008, **10**, 1724–1727.
26 Y. Hu, X. Li, D. Geng, M. Cai, R. Li and X. Sun, *Electrochim. Acta*, 2013, **91**, 227–233.
27 Z. Xin, C. M. Hayner, M. C. Kung and H. H. Kung, *ACS Nano*, 2011, **5**, 8739–8749.
28 M.-S. Balogun, F. Lyu, Y. Luo, W. Qiu, H. Meng, J. Li, W. Mai, L. Mai and Y. Tong, *Nano Energy*, 2016, **26**, 446–455.
29 J. Zhu, C. Tang, Z. Zhuang, C. Shi, N. Li, L. Zhou and L. Mai, *ACS Appl. Mater. Interfaces*, 2017, **9**, 24584–24590.
30 K. S. Novoselov, A. K. Geim, S. V. Morozov, D. Jiang, Y. Zhang, S. V. Dubonos, I. V. Grigorieva and A. A. Firsov, *Science*, 2004, **306**, 666–669.
31 P. Lian, J. Wang, D. Cai, L. Ding, Q. Jia and H. Wang, *Electrochim. Acta*, 2014, **116**, 103–110.
32 F. Y. Su, C. H. You, Y. B. He, L. Wei, C. Wei, F. M. Jin, B. H. Li, Q. H. Yang and F. Y. Kang, *J. Mater. Chem.*, 2010, **20**, 9644–9650.
33 Z. Tai, X. Yan, J. Lang and Q. Xue, *J. Power Sources*, 2012, **199**, 373–378.
34 D. Yang, W. Ni, J. Cheng, Z. Wang, T. Wang, Q. Guan, Y. Zhang, H. Wu, X. Li and B. Wang, *Appl. Surf. Sci.*, 2017, **413**, 209–218.
35 S. Bai, C. Sun, H. Yan, X. Sun, H. Zhang, L. Luo, X. Lei, P. Wan and X. Chen, *Small*, 2015, **11**, 5807–5813.
36 G. Fiori, F. Bonaccorso, G. Iannaccone, T. Palacios, D. Neumaier, A. Seabaugh, S. K. Banerjee and L. Colombo, *Nat. Nanotechnol.*, 2014, **9**, 768–779.
37 F. H. L. Koppens, T. Mueller, P. Avouris, A. C. Ferrari, M. S. Vitiello and M. Polini, *Nat. Nanotechnol.*, 2014, **9**, 780–793.
38 Y. Shuang, Y. Liu, C. Wen, J. Wei, Z. Jing, Z. Han, G. S. Zakharova and A. B. Chemical, *Sensors*, 2016, **226**, 478–485.
39 F. Xia, *Nat. Photonics*, 2014, **8**, 899–907.
40 Z. Guo, S. Chen, Z. Wang, Z. Yang, F. Liu, Y. Xu, J. Wang, Y. Yi, H. Zhang, L. Liao, P. K. Chu and X. F. Yu, *Adv. Mater.*, 2017, **29**, 1703811.

41 S. C. Dhanabalan, J. S. Ponraj, Z. Guo, S. Li, Q. Bao and H. Zhang, *Adv. Sci.*, 2017, **4**, 1600305.
42 D. Y. Tang, H. Zhang, L. M. Zhao, N. Xiang and X. Wu, *Opt. Express*, 2008, **16**, 9528–9533.
43 R. Cao, H. D. Wang, Z. N. Guo, D. K. Sang, L. Y. Zhang, Q. L. Xiao, Y. P. Zhang, D. Y. Fan, J. Q. Li and H. Zhang, *Adv. Opt. Mater.*, 2019, **7**, 1900020.
44 Y. Jiang, L. Miao, G. Jiang, Y. Chen, X. Qi, X. Jiang, H. Zhang and S. Wen, *Sci. Rep.*, 2015, **5**, 16372.
45 M. Liu, Z. R. Cai, S. Hu, A. P. Luo, C. J. Zhao, H. Zhang, W. C. Xu and Z. C. Luo, *Opt. Express*, 2015, **40**, 4767–4770.
46 Y. Song, Z. Liang, X. Jiang, Y. Chen, Z. Li, L. Lu, Y. Ge, K. Wang, J. Zheng and S. Lu, *2D Mater.*, 2017, **4**, 045010.
47 D. Tang, H. Zhang, L. Zhao and X. Wu, *Opt. Express*, 2010, **35**, 2756.
48 Y. Wang, F. Zhang, X. Tang, X. Chen, Y. Chen, W. Huang, Z. Liang, L. Wu, Y. Ge, Y. Song, J. Liu, D. Zhang, J. Li and H. Zhang, *Laser Photonics Rev.*, 2018, **12**, 1800016.
49 H. Zhang, D. Tang, L. Zhao and X. Wu, *Opt. Express*, 2011, **19**, 3525–3530.
50 L. M. Zhao, D. Y. Tang, H. Zhang, T. H. Cheng, H. Y. Tam and C. Lu, *Opt. Express*, 2007, **32**, 1806–1808.
51 H. Zhang, D. Y. Tang, L. M. Zhao and R. J. J. O. E. Knize, *Opt. Express*, 2010, **18**, 4428–4433.
52 H. Zhang, D. Y. Tang, H. Y. Tam and L. M. Zhao, *Opt. Express*, 2008, **33**, 2317–2319.
53 Q. Wang, Y. Chen, L. Miao, G. Jiang, S. Chen, J. Liu, X. Fu, C. Zhao and H. Zhang, *Opt. Express*, 2015, **23**, 7681–7693.
54 B. Wang, H. Yu, Z. Han, C. Zhao, S. Wen, H. Zhang and J. Wang, *IEEE Photonics J.*, 2014, **6**, 1501007.
55 M. Liu, X. W. Zheng, Y. L. Qi, H. Liu, A. P. Luo, Z. C. Luo, W. C. Xu, C. J. Zhao and H. Zhang, *Opt. Express*, 2014, **22**, 22841–22846.
56 J. Liu, Y. Chen, P. Tang, C. Xu, C. Zhao, H. Zhang and S. Wen, *Opt. Express*, 2015, **23**, 6418–6427.
57 L. Kong, Z. Qin, G. Xie, Z. Guo, H. Zhang, P. Yuan and L. Qian, *Laser Phys. Lett.*, 2016, **13**, 045801.
58 Y. Zhang, B. Lin, S. C. Tjin, H. Zhang, G. Wang, P. Shum and X. Zhang, *Opt. Express*, 2010, **18**, 26345–26350.
59 H. Zhang, D. Tang, L. Zhao, Q. Bao and K. P. Loh, *Opt. Commun.*, 2010, **283**, 3334–3338.
60 P. Yan, R. Lin, C. Hao, Z. Han, A. Liu, H. Yang and S. Ruan, *IEEE Photonics Technol. Lett.*, 2015, **27**, 264–267.
61 D. Y. Tang, L. M. Zhao, X. Wu and H. Zhang, *Phys. Rev. A*, 2009, **80**, 023806.
62 D. Y. Tang, H. Zhang, L. M. Zhao and X. Wu, *Opt. Express*, 2008, **16**, 10053–10058.
63 Y. F. Song, H. Zhang, D. Y. Tang and D. Y. Shen, *Opt. Express*, 2012, **20**, 27283–27289.
64 C. Yu, C. Zhao, S. Chen, J. Du, P. Tang, G. Jiang, Z. Han, S. Wen and D. Tang, *IEEE J. Sel. Top. Quantum Electron.*, 2014, **20**, 315–322.
65 Y. Ge, Z. Zhu, Y. Xu, Y. Chen, C. Si, Z. Liang, Y. Song, Y. Zou, H. Zeng and S. J. A. O. M. Xu, *Adv. Opt. Mater.*, 2017, **6**, 1701166.
66 L. Lu, Z. Liang, L. Wu, Y. X. Chen, Y. Song, S. C. Dhanabalan, J. S. Ponraj, B. Dong, Y. Xiang and F. Xing, *Laser Photonics Rev.*, 2018, **12**, 1700221.
67 L. Lu, X. Tang, R. Cao, L. Wu, Z. Li, G. Jing, B. Dong, S. Lu, Y. Li and Y. Xiang, *Adv. Opt. Mater.*, 2017, **5**, 1700301.
68 Y. Song, Y. Chen, X. Jiang, W. Liang, K. Wang, Z. Liang, Y. Ge, F. Zhang, L. Wu, J. Zheng, J. Ji and H. Zhang, *Adv. Opt. Mater.*, 2018, **6**, 1701287.
69 J. Shao, L. Tong, S. Tang, Z. Guo, H. Zhang, P. Li, H. Wang, C. Du and X. F. Yu, *ACS Appl. Mater. Interfaces*, 2015, **7**, 5391.
70 Q. Jiang, L. Xu, N. Chen, H. Zhang, L. Dai and S. Wang, *Angew. Chem., Int. Ed.*, 2016, **55**, 13849–13853.
71 M. Liu, N. Zhao, H. Liu and X. W. Zheng, *IEEE Photonics Technol. Lett.*, 2014, **26**, 983–986.
72 S. Bai, C. Sun, H. Yan, X. Sun, H. Zhang, L. Luo, X. Lei, P. Wan and X. Chen, *Small*, 2016, **11**, 5807–5813.
73 S. Yang, Y. Liu, C. Wen, J. Wei, Z. Jing, Z. Han and G. S. Zakharova, *Sens. Actuators, B*, 2016, **226**, 478–485.
74 P. Wan, X. Wen, C. Sun, B. K. Chandran, H. Zhang, X. Sun and X. Chen, *Small*, 2015, **11**, 5409–5415.
75 J. Shao, L. Tong, S. Tang, Z. Guo, H. Zhang, P. Li, H. Wang, C. Du and X. F. Yu, *ACS Appl. Mater. Interfaces*, 2015, **7**, 5391.
76 S. Chen, Z. Guo, D. K. Sang, H. Wang, Y. Xu, S. Tang, Q. Luo, R. Cao, X. Wang, L. Zhang, J. Liao, H. Zhang, X.-F. Yu, B. Zhao and D. Fan, *J. Raman Spectrosc.*, 2019, **50**, 26–33.
77 W. Tao, X. Ji, X. Xu, M. A. Islam, Z. Li, S. Chen, P. E. Saw, H. Zhang, Z. Bharwani and Z. Guo, *Angew. Chem., Int. Ed.*, 2017, **56**, 11896.
78 M. Qiu, D. Wang, W. Liang, L. Liu, Y. Zhang, X. Chen, D. K. Sang, C. Xing, Z. Li and B. Dong, *Proc. Natl. Acad. Sci. U. S. A.*, 2018, **115**, 501.
79 Z. Sun, Y. Zhao, Z. Li, H. Cui, Y. Zhou, W. Li, W. Tao, H. Zhang, H. Wang and P. K. Chu, *Small*, 2017, **13**, 1602896.
80 X. Ren, Z. Jie, Q. Xiang, Y. Liu, Z. Huang, Z. Li, Y. Ge, S. C. Dhanabalan, J. S. Ponraj and S. Wang, *Adv. Energy Mater.*, 2017, **7**, 1700396.
81 D. K. Sang, H. Wang, M. Qiu, R. Cao, Z. Guo, J. Zhao, Y. Li, Q. Xiao, D. Fan and H. Zhang, *Nanomaterials*, 2019, **9**, 82.
82 C. Xing, G. Jing, X. Liang, M. Qiu, Z. Li, R. Cao, X. Li, D. Fan and H. J. N. Zhang, *Nanoscale*, 2017, **9**, 8096–8101.
83 J. Li, H. Luo, B. Zhai, R. Lu, Z. Guo, H. Zhang and Y. Liu, *Sci. Rep.*, 2016, **6**, 30361.
84 Y. Xu, X. F. Jiang, Y. Ge, Z. Guo, Z. Zeng, Q. H. Xu, Z. Han, X. F. Yu and D. Fan, *J. Mater. Chem. C*, 2017, **5**, 3007.
85 Y. Tao, T. Huang, C. Ding, F. Yu, D. Tan, F. Wang, Q. Xie and S. Yao, *Appl. Mater. Today*, 2019, **15**, 18–33.
86 J. Carrete, L. Wu, L. Lindsay, D. A. Broido, L. J. Gallego and N. Mingo, *Mater. Res. Lett.*, 2017, **18**, 204–211.
87 B. Mortazavi, O. Rahaman, S. Ahzi and T. Rabczuk, *Appl. Mater. Today*, 2017, **8**, 60–67.
88 M. Denk, R. Lennon, R. Hayashi, R. West, A. V. Belyakov, H. P. Verne, A. Haaland, M. Wagner and N. Metzler, *J. Am. Chem. Soc.*, 1994, **116**, 2691–2692.
89 L. Linfei, L. Shuang-Zan, P. Jinbo, Q. Zhihui, W. Yu-Qi, W. Yeliang, C. Geng-Yu, D. Shixuan and G. Hong-Jun, *Adv. Mater.*, 2014, **26**, 4820–4824.
90 F. F. Zhu, W. J. Chen, Y. Xu, C. L. Gao, D. D. Guan, C. H. Liu, D. Qian, S. C. Zhang and J. F. Jia, *Nat. Mater.*, 2015, **14**, 1020–1025.

91 J. Lu, K. Zhang, X. Feng Liu, H. Zhang, T. Chien Sum, A. H. Castro Neto and K. P. Loh, *Nat. Commun.*, 2013, **4**, 2618.
92 M. Naguib, M. Kurtoglu, V. Presser, J. Lu, J. Niu, M. Heon, L. Hultman, Y. Gogotsi and M. W. Barsoum, *Adv. Mater.*, 2011, **23**, 4248–4253.
93 M. Naguib, V. N. Mochalin, M. W. Barsoum and Y. Gogotsi, *Adv. Mater.*, 2014, **26**, 992–1005.
94 Y. Chen, M. Wu, P. Tang, S. Chen, J. Du, G. Jiang, Y. Li, C. Zhao, H. Zhang and S. Wen, *Laser Phys. Lett.*, 2014, **11**, 055101.
95 Q. Wu, S. Chen, Y. Wang, L. Wu, X. Jiang, F. Zhang, X. Jin, Q. Jiang, Z. Zheng, J. Li, M. Zhang and H. Zhang, *Adv. Mater. Technol.*, 2019, **4**, 1800532.
96 X. Jiang, S. Liu, W. Liang, S. Luo, Z. He, Y. Ge, H. Wang, C. Rui, Z. Feng and W. J. L. Qiao, *Laser Photonics Rev.*, 2017, **12**, 1700229.
97 S. Tongay, J. Zhou, C. Ataca, K. Lo, T. S. Matthews, J. Li, J. C. Grossman and J. Wu, *Nano Lett.*, 2015, **12**, 5576–5580.
98 Y. Ge, Z. Zhu, Y. Xu, Y. Chen, C. Si, Z. Liang, Y. Song, Y. Zou, H. Zeng and S. Xu, *Adv. Opt. Mater.*, 2017, **6**, 1701166.
99 L. Yang, K. Majumdar, H. Liu, Y. Du, H. Wu, M. Hatzistergos, P. Y. Hung, R. Tieckelmann, W. Tsai and C. Hobbs, *Nano Lett.*, 2014, **14**, 6275.
100 A. Sajedi-Moghaddam, C. C. Mayorga-Martinez, E. Saievar-Iranizad, Z. Sofer and M. Pumera, *Appl. Mater. Today*, 2019, **16**, 280–289.
101 J. Heising and M. G. Kanatzidis, *J. Am. Chem. Soc.*, 1999, **121**, 11720–11732.
102 A. K. Geim and K. S. Novoselov, *Nat. Mater.*, 2007, **6**, 183–191.
103 H. S. S. R. Matte, A. Gomathi, A. Manna, D. Late, R. Datta, S. Pati and C. N. R. Rao, *Angew. Chem., Int. Ed.*, 2010, **49**, 4059–4062.
104 U. K. Sen and S. Mitra, *RSC Adv.*, 2012, **2**, 11123–11131.
105 J. Huang, M. A. Renzhi, E. Yasuo, F. Katsutoshi, T. Kazunori and S. Takayoshi, *Chem. Mater.*, 2010, **22**, 2582–2587.
106 X. Y. Xue, B. He, S. Yuan, L. L. Xing, Z. H. Chen and C. H. Ma, *Nanotechnology*, 2011, **22**, 395702.
107 K. Ma, X. Liu, Q. Cheng, P. Saha, H. Jiang and C. Li, *J. Power Sources*, 2017, **357**, 71–76.
108 D. Su and G. Wang, *ACS Nano*, 2013, **7**, 11218–11226.
109 G. Sansone, A. J. Karttunen, D. Usvyat, M. Schutz, J. G. Brandenburg and L. Maschio, *Chem. Commun.*, 2018, **54**, 9793–9796.
110 J. Guan, Z. Zhu and D. Tomanek, *Phys. Rev. Lett.*, 2014, **113**, 226801.
111 J. S. Kang, M. Ke and Y. Hu, *Nano Lett.*, 2017, **17**, 1431–1438.
112 L. Q. Sun, M. J. Li, K. Sun, S. H. Yu, R. S. Wang and H. M. Xie, *J. Phys. Chem. C*, 2012, **116**, 14772–14779.
113 J. Qiao, X. Kong, Z. X. Hu, F. Yang and W. Ji, *Nat. Commun.*, 2014, **5**, 4475.
114 L. Li, Y. Yu, G. J. Ye, Q. Ge, X. Ou, H. Wu, D. Feng, X. H. Chen and Y. Zhang, *Nat. Nanotechnol.*, 2014, **9**, 372–377.
115 Z. Pang, Q. Xin, Y. Wei and R. Yang, *Europhys. Lett.*, 2016, **116**, 36001.
116 H. R. Jiang, Z. Lu, M. C. Wu, F. Ciucci and T. S. Zhao, *Nano Energy*, 2016, **23**, 97–104.
117 B. Mortazavi, A. Dianat, G. Cuniberti and T. I. Rabczuk, *Electrochim. Acta*, 2016, **213**, 865–870.
118 X. Li, J. T. Mullen, Z. Jin, K. M. Borysenko, M. B. Nardelli and K. W. Kim, *Phys. Rev. B: Condens. Matter Mater. Phys.*, 2013, **87**, 115418.
119 P. Yu, G. Cao, S. Yi, X. Zhang, C. Li, X. Sun, K. Wang and Y. Ma, *Nanoscale*, 2018, **10**, 5906.
120 A. Lipatov, M. Alhabeb, M. R. Lukatskaya, A. Boson, Y. Gogotsi and A. Sinitskii, *Adv. Electron. Mater.*, 2016, **2**, 1600255.
121 M. R. Gao, M. K. Y. Chan and Y. Sun, *Nat. Commun.*, 2015, **6**, 7493.
122 T. Stephenson, Z. Li, B. Olsen and D. Mitlin, *Energy Environ. Sci.*, 2013, **7**, 209–231.
123 B. Radisavljevic, A. Radenovic, J. Brivio, V. Giacometti and A. Kis, *Nat. Nanotechnol.*, 2011, **6**, 147–150.
124 B. Feng, Z. Ding, S. Meng, Y. Yao, X. He, P. Cheng, L. Chen and K. Wu, *Nano Lett.*, 2012, **12**, 3507–3511.
125 G. Huang, L. Hao, S. Wang, Y. Xi, B. Liu, H. Chen and M. Xu, *J. Mater. Chem. A*, 2015, **3**, 24128–24138.
126 K. Shiva, H. S. S. R. Matte, H. B. Rajendra, A. J. Bhattacharyya and C. N. R. Rao, *Nano Energy*, 2013, **2**, 787–793.
127 W. Zhang, Z. Huang, W. Zhang and Y. Li, *Nano Res.*, 2014, **7**, 1731–1737.
128 J. Shin, H. Jung, Y. Kim and J. Kim, *J. Alloys Compd.*, 2014, **589**, 322–329.
129 F. K. Butt, C. Cao, F. Idrees, M. Tahir, R. Hussain and A. Z. Alshemary, *New J. Chem.*, 2015, **39**, 5197–5202.
130 R. Enjalbert and J. Galy, *Acta Crystallogr., Sect. C: Struct. Chem.*, 2014, **42**, 1467–1469.
131 C. Tan, X. Cao, X. J. Wu, Q. He, J. Yang, X. Zhang, J. Chen, W. Zhao, S. Han and G. H. Nam, *Chem. Rev.*, 2017, **117**, 6225–6331.
132 C.-M. Park and H. J. Sohn, *ChemInform*, 2007, **19**, 2465–2468.
133 Q. Tang, Z. Zhou and P. Shen, *J. Am. Chem. Soc.*, 2012, **134**, 16909.
134 P. Xiang, X. Zhang, W. Lei, L. Hu, H. S. Cheng, H. Chao, B. Gao, M. Fei, K. Huo and P. K. Chu, *Adv. Funct. Mater.*, 2016, **26**, 784–791.
135 X. Zhang, J. Hu, Y. Cheng, H. Y. Yang, Y. Yao and S. A. Yang, *Nanoscale*, 2016, **8**, 15340–15347.
136 A. J. Mannix, X.-F. Zhou, B. Kiraly, J. D. Wood, D. Alducin, B. D. Myers, X. Liu, B. L. Fisher, U. Santiago and J. R. Guest, *Science*, 2016, **350**, 1513.
137 B. Peng, H. Zhang, H. Shao, Y. Xu, R. Zhang and H. Zhu, *J. Mater. Chem. C*, 2016, **4**, 3592–3598.
138 Y. Xu, X. F. Jiang, Y. Ge, Z. Guo, Z. Zeng, Q. H. Xu, H. Zhang, X. F. Yu and D. Fan, *J. Mater. Chem. C*, 2017, **5**, 3007–3013.
139 Q. Wei and X. Peng, *Appl. Phys. Lett.*, 2014, **104**, 251915.
140 C. Lee, X. Wei, J. W. Kysar and J. Hone, *Science*, 2008, **321**, 385–388.
141 Z. Zhang, Y. Yang, E. S. Penev and B. I. Yakobson, *Adv. Funct. Mater.*, 2016, **27**, 1605059.

142 R. E. Roman and S. W. Cranford, *Comput. Mater. Sci.*, 2014, **82**, 50–55.
143 H. Tian, Z. W. Seh, K. Yan, Z. Fu, P. Tang, Y. Lu, R. Zhang, D. Legut, Y. Cui and Q. Zhang, *Adv. Energy Mater.*, 2017, **7**, 1602528.
144 A. Lipatov, H. Lu, M. Alhabeb, B. Anasori, A. Gruverman, Y. Gogotsi and A. Sinitskii, *Sci. Adv.*, 2018, **4**, eaat0491.
145 Z. Guo, J. Zhou, C. Si and Z. Sun, *Phys. Chem. Chem. Phys.*, 2015, **17**, 15348–15354.
146 S. Bertolazzi, J. Brivio and A. Kis, *ACS Nano*, 2011, **5**, 9703–9709.
147 A. Castellanos-Gomez, M. Poot, G. A. Steele, H. S. J. V. D. Zant, N. Agraït and G. Rubio-Bollinger, *Adv. Mater.*, 2012, **24**, 772–775.
148 N. Fateh, G. A. Fontalvo and C. Mitterer, *J. Phys. D: Appl. Phys.*, 2007, **40**, 7716.
149 J. Du, V. C. Anye, E. O. Vodah, T. Tong, M. G. Z. Kana and W. O. Soboyejo, *J. Appl. Phys.*, 2014, **115**, 429–433.
150 Y. Chen, G. Jiang, S. Chen, Z. Guo, X. Yu, C. Zhao, H. Zhang, Q. Bao, S. Wen, D. Tang and D. Fan, *Opt. Express*, 2015, **23**, 12823–12833.
151 W. Lu, H. Nan, J. Hong, Y. Chen, C. Zhu, Z. Liang, X. Ma, Z. Ni, C. Jin and Z. Zhang, *Nano Res.*, 2014, **7**, 853–859.
152 H. Li, J. Wu, Z. Yin and H. Zhang, *Acc. Chem. Res.*, 2014, **47**, 1067–1075.
153 Y. Zhao, X. Luo, H. Li, J. Zhang, P. T. Araujo, C. K. Gan, J. Wu, H. Zhang, S. Y. Quek and M. S. Dresselhaus, *Nano Lett.*, 2013, **13**, 1007–1015.
154 H. Li, G. Lu, Y. Wang, Z. Yin, C. Cong, Q. He, L. Wang, F. Ding, T. Yu and H. Zhang, *Small*, 2013, **9**, 1974–1981.
155 L. Gang and N. Komatsu, *ChemNanoMat*, 2016, **2**, 500–503.
156 H. Liu, A. T. Neal, Z. Zhu, Z. Luo, X. Xu, D. Tománek and P. D. Ye, *ACS Nano*, 2014, **8**, 4033–4041.
157 A. Castellanos-Gomez, L. Vicarelli, E. Prada, J. O. Island, K. L. Narasimha-Acharya, S. I. Blanter, D. J. Groenendijk, M. Buscema, G. A. Steele and J. V. Alvarez, *2D Mater.*, 2014, **1**, 025001.
158 V. Nicolosi, M. Chhowalla, M. G. Kanatzidis, M. S. Strano and J. N. Coleman, *Science*, 2013, **340**, 1226419.
159 D. Hanlon, C. Backes, E. Doherty, C. S. Cucinotta, N. C. Berner, C. Boland, C. Boland, K. Lee, A. Harvey, P. Lynch, Z. Gholamvand, S. Zhang, K. Wang, G. Moynihan, G. Pokle, Q. M. Ramasse, N. McEvoy, W. J. Blau, J. Wang, G. Abellan, F. Hauke, A. Hirsch, S. Sanvito, D. D. O'Regan, G. S. Duesberg, V. Nicolosi and J. N. Coleman, *Sci. Rep.*, 2015, **6**, 8563.
160 J. R. Brent, S. Nicky, E. A. Lewis, S. J. Haigh, D. J. Lewis and O. B. Paul, *Chem. Commun.*, 2014, **50**, 13338–13341.
161 Z. Guo, H. Zhang, S. Lu, Z. Wang and P. K. Chu, *Adv. Funct. Mater.*, 2015, **25**, 6996–7002.
162 Y. Xu, Z. Wang, Z. Guo, H. Huang, Q. Xiao, H. Zhang and X. Yu, *Adv. Opt. Mater.*, 2016, **4**, 1223–1229.
163 G. S. Bang, K. W. Nam, J. Y. Kim, J. Shin, J. W. Choi and S. Y. Choi, *ACS Appl. Mater. Interfaces*, 2014, **6**, 7084–7089.
164 E. P. Nguyen, B. J. Carey, T. Daeneke, J. Z. Ou, K. Latham, S. Zhuiykov and K. Kalantar-zadeh, *Chem. Mater.*, 2015, **27**, 53–59.
165 C. Zhang, H. P. Sang, S. E. O'Brien, A. Seral-Ascaso, M. Liang, D. Hanlon, D. Krishnan, A. Crossley, N. Mcevoy and J. N. Coleman, *Nano Energy*, 2017, **39**, 151–161.
166 B. Mendozasánchez, D. Hanlon, J. Coelho, S. O'Brien, H. Pettersson, J. Coleman and V. Nicolosi, *2D Mater.*, 2016, **4**, 015005.
167 R. S. Datta, F. Haque, M. Mohiuddin, B. J. Carey, N. Syed, A. Zavabeti, B. Zhang, H. Khan, K. J. Berean and J. Z. Ou, *J. Mater. Chem. A*, 2017, **5**, 24223–24231.
168 O. Mashtalir, M. Naguib, B. Dyatkin, Y. Gogotsi and M. W. Barsoum, *Mater. Chem. Phys.*, 2013, **139**, 147–152.
169 L. H. Karlsson, J. Birch, J. Halim, M. W. Barsoum and P. O. Persson, *Nano Lett.*, 2015, **15**, 4955.
170 L. Wang, H. Zhang, W. Bo, C. Shen, C. Zhang, Q. Hu, A. Zhou and B. Liu, *Electron. Mater. Lett.*, 2016, **12**, 702–710.
171 P. Urbankowski, B. Anasori, T. Makaryan, D. Er and Y. Gogotsi, *Nanoscale*, 2016, **8**, 11385–11391.
172 Z. Yi, L. Gomez, F. N. Ishikawa, A. Madaria and C. Zhou, *J. Phys. Chem. Lett.*, 2015, **1**, 3101–3107.
173 J. B. Smith, D. Hagaman and H. F. Ji, *Nanotechnology*, 2016, **27**, 215602.
174 I. S. Kim, V. K. Sangwan, D. Jariwala, J. D. Wood, S. Park, K. S. Chen, F. Shi, F. Ruiz-Zepeda, A. Ponce, M. Jose-Yacaman, V. P. Dravid, T. J. Marks, M. C. Hersam and L. J. Lauhon, *ACS Nano*, 2014, **8**, 10551–10558.
175 H. Xia, H. Li, C. Lan, C. Li and Y. Liu, *Opt. Express*, 2014, **22**, 17341–17348.
176 J. Jaeho, J. Sung Kyu, J. S. Min, Y. Gwangwe, J. Y. Hee, P. Jin-Hong and L. Sungjoo, *Nanoscale*, 2014, **7**, 1688–1695.
177 S. Lee, J. Kim, J. H. Jeon, M. Song, S. Kim, Y. G. You, S. H. Jhang, S. A. Seo and S. H. Chun, *ACS Appl. Mater. Interfaces*, 2018, **10**, 42875–42881.
178 K. K. Wang, F. X. Wang, Y. D. Liu and G. B. Pan, *Mater. Lett.*, 2013, **102–103**, 8–11.
179 L. Chen, G. Zhou, Z. Liu, X. Ma, J. Chen, Z. Zhang, X. Ma, F. Li, H. M. Cheng and W. Ren, *Adv. Mater.*, 2016, **28**, 510–517.
180 D. Li, D. Wang, K. Rui, Z. Ma, L. Xie, J. Liu, Y. Zhang, R. Chen, Y. Yan, H. Lin, X. Xie, J. Zhu and W. Huang, *J. Power Sources*, 2018, **384**, 27–33.
181 Q. Peng, Z. Wang, B. Sa, B. Wu and Z. Sun, *ACS Appl. Mater. Interfaces*, 2016, **8**, 13449–13457.
182 Q. Peng, K. Hu, B. Sa, J. Zhou, B. Wu, X. Hou and Z. Sun, *Nano Res.*, 2017, **10**, 3136–3150.
183 Z. Ling, C. E. Ren, M. Zhao, J. Yang, G. M. James, J. Qiu, B. W. Michel and Y. Gogotsi, *Proc. Natl. Acad. Sci. U. S. A.*, 2014, **111**, 16676–16681.
184 M. Q. Zhao, M. Torelli, C. E. Ren, M. Ghidiu, Z. Ling, B. Anasori, M. W. Barsoum and Y. Gogotsi, *Nano Energy*, 2016, **30**, 603–613.
185 A. Byeon, M.-Q. Zhao, C. E. Ren, J. Halim, S. Kota, P. Urbankowski, B. Anasori, M. W. Barsoum and Y. Gogotsi, *ACS Appl. Mater. Interfaces*, 2017, **9**, 4296–4300.
186 Y. Liu, W. Wang, Y. Ying, Y. Wang and X. Peng, *Dalton Trans.*, 2015, **44**, 7123–7126.
187 C. Zhao, J. Kong, X. Yao, X. Tang, Y. Dong, S. L. Phua and X. Lu, *ACS Appl. Mater. Interfaces*, 2014, **6**, 6392–6398.

188 Z. Deng, H. Jiang, Y. Hu, Y. Liu and C. Li, *Adv. Mater.*, 2017, **29**, 1603020.
189 H. Yu, C. Zhu, K. Zhang, Y. Chen, C. Li, P. Gao, P. Yang and Q. Ouyang, *J. Mater. Chem. A*, 2014, **2**, 4551.
190 Z. Wang, M. Liu, G. Wei, P. Han, X. Zhao, J. Liu, Y. Zhou and J. Zhang, *Appl. Surf. Sci.*, 2017, **423**, 375–382.
191 Y. Liu, W. Wang, H. Huang, L. Gu, Y. Wang and X. Peng, *Chem. Commun.*, 2014, **50**, 4485–4488.
192 W. Chen, X. Zeng, P. He, L. Chen and W. Wei, *Adv. Mater. Interfaces*, 2017, **5**, 1701080.
193 L. Zhang, W. Fan and T. Liu, *Nanoscale*, 2016, **8**, 16387.
194 L. Zhi, D. Kong, Y. Zhang, X. Li and Q. H. Yang, *Energy Environ. Sci.*, 2016, **9**, 906–911.
195 B. Feng, J. Zhang, Q. Zhong, W. Li, S. Li, H. Li, P. Cheng, S. Meng, L. Chen and K. Wu, *Nat. Chem.*, 2016, **8**, 563–568.
196 H. Mu, Z. Wang, Y. Jian, X. Si, C. Chen, C. Yu, C. Yao, J. Song, Y. Wang and Y. Xue, *ACS Photonics*, 2015, **2**, 832.
197 Z. Li, Q. Hui, Z. Guo, X. Ren, Z. Huang, Q. Xiang, S. C. Dhanabalan, J. S. Ponraj, Z. Du and J. Li, *Adv. Funct. Mater.*, 2017, **28**, 1705237.
198 J. Lu, Z. Kai, F. L. Xin, Z. Han, T. C. Sum, A. H. C. Neto and K. P. Loh, *Nat. Commun.*, 2013, **4**, 2681.
199 D. K. Sang, H. Wang, M. Qiu, R. Cao, Z. Guo, J. Zhao, Y. Li, Q. Xiao, D. Fan and H. Zhang, *Nanomaterials*, 2019, **9**, 82.
200 H. Xie, Z. Li, Z. Sun, J. Shao, X. F. Yu, Z. Guo, J. Wang, Q. Xiao, H. Wang, Q.-Q. Wang, H. Zhang and P. K. Chu, *Small*, 2016, **12**, 4136–4145.
201 K. S. Novoselov, A. Mishchenko, A. Carvalho and A. H. C. Neto, *Science*, 2016, **353**, 9439.
202 Y. Shi, W. Zhou, A. Y. Lu, W. Fang, Y. H. Lee, A. L. Hsu, S. M. Kim, K. K. Kim, H. Y. Yang, L. J. Li, J. C. Idrobo and J. Kong, *Nano Lett.*, 2012, **12**, 2784–2791.
203 G. S. Duesberg, *Nat. Mater.*, 2014, **13**, 1075.
204 X. Chen, Y. Qiu, H. Yang, G. Liu, W. Zheng, W. Feng, W. Cao, W. Hu and P. Hu, *ACS Appl. Mater. Interfaces*, 2017, **9**, 1684–1691.
205 W. Shanshan, W. Xiaochen and J. H. Warner, *ACS Nano*, 2015, **9**, 5246.
206 L. Britnell and K. S. Novoselov, *Science*, 2013, **340**, 1311–1314.
207 C. Wang, Q. He, U. Halim, Y. Liu, Z. Enbo, Z. Lin, H. Xiao, X. Duan, Z. Feng, R. Cheng, N. O. Weiss, G. Ye, Y.-C. Huang, H. Wu, H.-C. Cheng, I. Shakir, L. Liao, X. Chen, W. A. Goddard III, Y. Huang and X. Duan, *Nature*, 2018, **555**, 231–236.
208 Y. Ge, S. Chen, Y. Xu, Z. He, Z. Liang, Y. Chen, Y. Song, D. Fan, K. Zhang and H. Zhang, *J. Mater. Chem. C*, 2017, **5**, 6129–6135.
209 C. Xing, G. Jing, X. Liang, M. Qiu, Z. Li, R. Cao, X. Li, D. Fan and H. Zhang, *Nanoscale*, 2017, **9**, 8096.
210 X. Ren, Z. Li, Z. Huang, D. Sang, H. Qiao, X. Qi, J. Li, J. Zhong and H. Zhang, *Adv. Funct. Mater.*, 2017, **27**, 1606834.
211 S. Y. Choi, Y. Kim, H.-S. Chung, A. R. Kim, J.-D. Kwon, J. Park, Y. L. Kim, S.-H. Kwon, M. G. Hahm and B. Cho, *ACS Appl. Mater. Interfaces*, 2017, **9**, 3817–3823.
212 D. H. Wu, S. Wang, S. Zhang, Y. Liu and H. Chen, *Phys. Chem. Chem. Phys.*, 2018, **21**, 1029–1037.